

Convergence of the Embedded Mean-Variance Optimal Points With Discrete Sampling*

Duy-Minh Dang [†] Peter A. Forsyth [‡] Yuying Li [§]

March 8, 2016

Abstract

A numerical technique based on the embedding technique proposed in [21, 33] for dynamic mean-variance (MV) optimization problems may yield spurious points, i.e. points which are not on the efficient frontier. In [27], it is shown that spurious points can be eliminated by examining the left upper convex hull of the solution of the embedded problem. However, any numerical algorithm will generate only a discrete sampling of the solution set of the embedded problem. In this paper, we formally establish that, under mild assumptions, every limit point of a suitably defined sequence of upper convex hulls of the sampled solution of the embedded problem is on the original MV efficient frontier. For illustration, we discuss an MV asset-liability problem under jump diffusions, which is solved using a numerical Hamilton-Jacobi-Bellman partial differential equation approach.

Keywords: mean-variance, scalarization optimization, embedding, Pareto optimal, asset-liability, Hamilton-Jacobi-Bellman (HJB) equation, jump diffusion

AMS Classification: 65K29, 91G60, 93C20

1 Introduction

The main objective of this paper is to analyze convergence properties of the computed mean-variance (MV) scalarization optimal points, sequenced by the embedding parameter sampling level, in the embedding technique for multi-period MV optimization.

1.1 Motivation

Many optimal stochastic control problems in finance can be formulated as a multi-period or continuous time MV optimization problem. Typical examples include portfolio optimization [7, 21, 25, 28, 29, 33], asset-liability management [5, 10, 15, 19, 20, 31], and optimal trade execution[17, 23].

*This work was supported by the Natural Sciences and Engineering Research Council (NSERC) of Canada, and by a Credit Suisse Research Grant. The views expressed herein are solely those of the authors, and not those of any other person or entity, including Credit Suisse.

[†]School of Mathematics and Physics, The University of Queensland, Brisbane, QLD 4072, Australia
duyminh.dang@uq.edu.au

[‡]David R. Cheriton School of Computer Science, University of Waterloo, Waterloo ON, Canada N2L 3G1
paforsyt@uwaterloo.ca

[§]David R. Cheriton School of Computer Science, University of Waterloo, Waterloo ON, Canada N2L 3G1
yuying@uwaterloo.ca

27 In this approach, we seek the optimal trade-off between the two conflicting criteria of maximizing
28 the expected wealth of the investment (or trading), over a given time horizon, and minimizing
29 investment risk. More specifically, letting W_t denote the total wealth from the investment at
30 time t , we aim to maximize $\mathcal{E} = E[W_T]$ and minimize $\mathcal{V} = Var[W_T]$, where T is the end of the
31 investment/trading horizon. Here, $E[\cdot]$ and $Var[\cdot]$ respectively denote the expectation and the
32 variance operators.

33 Mean-variance optimization typically yields pre-commitment strategies [4, 8], which are not
34 time-consistent [28, 29, 30]. There has been much discussion about such strategies in the economics
35 literature [8]. However, it is argued in [28] that pre-commitment strategies are appropriate in the
36 context of pension plan investment. It has also been pointed out that, in the context of optimal trade
37 execution, the pre-commitment strategy optimizes trading efficiency as measured in practice [1].
38 The pre-commitment policy has also been commonly applied in insurance applications [9, 15, 19, 32].

39 As an illustration to relevant issues addressed in this paper, we consider the following applica-
40 tion. Consider an investor who has a fixed initial wealth, which can be invested in (i) a risk-free
41 asset, e.g., a government bond, or (ii) a risky asset, e.g., a stock market index. We assume that the
42 investor can dynamically transfer wealth between these two assets. In addition to these assets, we
43 assume that the investor also has fixed liabilities, in the form of deterministic cash outflows. These
44 cash outflows are withdrawn at a set of pre-determined (event) dates. These cash outflows are
45 usually specified in terms of an initial withdrawal and subsequent withdrawals equal to the initial
46 withdrawal inflated at a known inflation rate. This asset-liability problem is assumed to continue
47 over a relatively long horizon, e.g. 20 years.

48 The problem described above can be viewed as a prototype for the asset allocation problem,
49 faced by the holder of a defined contribution pension plan (DCPP) in the sense that, upon retire-
50 ment, the holder of a DCPP must invest his assets to generate living expenses over a long term
51 horizon. Most existing literature for DCPP adopts an utility function based approach, see e.g., [28]
52 and references therein. This may be partly due to the fact that it is more challenging to numerically
53 determine the dynamic investment strategy which is optimal in the MV sense. As another concrete
54 example, we can consider the case of a charitable endowment, where fixed cash flows (i.e. staff
55 salaries) must be funded by an endowment which is invested in risky assets.

56 In both cases, the investment strategy can be modeled as a fraction of the total wealth invested
57 in the risky asset. In the example considered in this paper, we assume that the underlying risky
58 asset follows a jump diffusion process and we constrain the leverage ratio. To the best of our
59 knowledge, no closed-form solutions for this problem are presently available in the literature.

60 1.2 Background

61 Following a standard scalarization method for multi-criteria optimization, a single criterion can be
62 formed by a positively weighted sum of the criteria. Unfortunately, in the case of MV optimiza-
63 tion, dynamic programming is not directly applicable to the resulting single-objective optimization
64 problem, due to the presence of the variance term $Var[W_T]$.

65 1.2.1 Embedding Approach

66 To overcome this difficulty, a technique is proposed in [21, 33] to embed the objective of the MV
67 scalarization problem in a new optimization problem, which involves $\mathcal{E} = E[W_T]$, $\mathcal{Q} = E[W_T^2]$, and
68 an embedding parameter $\gamma \in (-\infty, +\infty)$, instead of \mathcal{E} , \mathcal{V} , and a positive scalarization parameter

69 $\mu > 0$. The dynamic programming principle can be applied to the embedded optimization problem,
70 which gives rise to a non-linear Hamilton-Jacobi-Bellman (HJB) equation, from which optimal
71 solutions with respect to the embedded problem can be obtained. For each embedding parameter
72 γ , a pair $(\mathcal{E}, \mathcal{V})$ of values is associated with a solution to the corresponding HJB equation, see, e.g.,
73 [13, 17, 29].

74 We denote by \mathcal{Y}_P the set of all $(\mathcal{V}, \mathcal{E})$ corresponding to the original MV scalarization problem.
75 We will also refer to \mathcal{Y}_P as the set of scalarization optimal points (SOPs) w.r.t. \mathcal{Y} . Let \mathcal{Y}_Q be the
76 set of all achievable $(\mathcal{V}, \mathcal{E})$ whose combination using an embedding parameter γ yields the optimal
77 value of the embedded problem with the embedding parameter γ . Our goal is to determine the set
78 \mathcal{Y}_P numerically. It has been established in [21, 33] that the original MV scalarization optimal set
79 \mathcal{Y}_P is a subset of the embedded MV objective set \mathcal{Y}_Q . This result has led to widespread adoption
80 of the embedding technique in MV optimization.

81 Unfortunately, the result that $\mathcal{Y}_P \subset \mathcal{Y}_Q$ is insufficient by itself, since there may exist *spurious*
82 points, i.e., points in \mathcal{Y}_Q but not in \mathcal{Y}_P . This problem can arise from nonconvexity of the original
83 problem. Furthermore a point in \mathcal{Y}_Q is a point in \mathcal{Y}_P only for an embedding parameter satisfying
84 necessary conditions. It is however difficult to verify these conditions in numerical computation;
85 consequently a method for eliminating spurious points is required. Note that the imposition of the
86 necessary conditions is not an issue when closed form solutions are available since the necessary
87 conditions can be imposed explicitly (e.g. see [33]).

88 The issue of potential spurious points for the embedding method in the context of numerical
89 computation was discussed in [27]. This raises an important issue of how to develop an algorithm for
90 eliminating these points. This issue is partially addressed in [27] by identification of scalarization
91 optimal points with respect to the embedded MV objective set. Specifically, it is shown that a
92 spurious point is a point at which a supporting hyperplane for the embedded MV objective set
93 does not exist, i.e. non-SOPs.

94 It is further noted in [27] that the full embedded objective set is not available in computation,
95 since any numerical algorithm can compute only a single MV point corresponding to a given em-
96 bedding γ . As a result, the requirement of constructing the full embedded MV set is relaxed, and
97 the focus is on the computed objective set [27]. The *computed* embedded MV objective set \mathcal{Y}_Q^\dagger
98 is defined as the embedded MV objective set with a single embedded MV objective point for each
99 embedding parameter. It is shown in [27] that the spurious points are non-SOPs with respect to
100 the computed MV set \mathcal{Y}_Q^\dagger . These theoretical results yield a post-processing technique for the em-
101 bedding method. This technique is applied to remove spurious points, which are now points in \mathcal{Y}_Q^\dagger
102 but not in \mathcal{Y}_P . This requires verification of the existence of a supporting hyperplane at each point
103 in the set \mathcal{Y}_Q^\dagger , and hence, has a simple geometrical interpretation. We denote by $\mathcal{S}(\mathcal{Y}_Q^\dagger)$ the set of
104 points in \mathcal{Y}_Q^\dagger at which supporting hyperplanes exist. The main result in [27] is that $\mathcal{S}(\mathcal{Y}_Q^\dagger) = \mathcal{Y}_P$.

105 1.2.2 Alternative Approaches

106 There are several other techniques which can be used to circumvent the problem due to the variance
107 term in MV optimization. A Martingale method, which is based on the use of Backward Stochastic
108 Differential Equations (BSDEs) was used in [7]. Another method, also using BSDEs, is described
109 in [12]. This technique is based on requiring that the admissible strategies satisfy a cone constraint.
110 Unfortunately, in practice, constraints which can not be expressed as a cone constraint may also
111 need to be imposed.

112 Finally, the method most closely related to the embedding method is based on using a Lagrange
 113 multiplier technique [11, 22]. Formally, this method requires that the problem can be posed as a
 114 convex optimization problem. This cannot be guaranteed in the case of the optimal execution
 115 problem discussed in [27], where the differential equations describing the underlying processes are
 116 nonlinear. It is interesting to observe that the final objective function in the Lagrange multiplier
 117 method has the same algebraic structure as the objective function in the embedding method.

118 1.3 Contributions of this paper

119 Although the theoretical results in [27] are important and practically useful, there is one additional
 120 complication which has not been addressed: it is computationally infeasible to compute the entire
 121 set \mathcal{Y}_Q^\dagger , since the embedding parameter $\gamma \in (-\infty, +\infty)$. In practice, we can only compute a solution
 122 of the embedded optimization problem for a set of finitely sampled embedding parameter values.
 123 Assume that $\Gamma_k \subset (-\infty, +\infty)$ is the set of sampled γ values at the sampling discretization level k ,
 124 and denote the MV finite set corresponding to Γ_k by $(\mathcal{Y}_Q^\dagger)^k$. We assume that the index k is positively
 125 proportional to the number of finite values of γ used in computation. A conjecture made in [27]
 126 is that any reasonable finite sampling method for γ , such as systematically refining uniform grids,
 127 results in the set $\mathcal{S}((\mathcal{Y}_Q^\dagger)^k)$ converging to, possibly a subset of, the set $\mathcal{S}(\mathcal{Y}_Q^\dagger)$ (or equivalently, the set
 128 \mathcal{Y}_P). However, this is by no means obvious, due to the fact that we use supporting hyperplanes of
 129 $(\mathcal{Y}_Q^\dagger)^k$ to determine $\mathcal{S}((\mathcal{Y}_Q^\dagger)^k)$. Given the importance of the embedding technique and its popularity
 130 in multi-period MV optimization, it is highly desirable to mathematically establish the validity of
 131 this conjecture. In other words, it is necessary to analyze asymptotic properties of SOPs with
 132 respect to the discretization of the embedding parameter. As a result, we can develop a post-
 133 processing technique for the computed $(\mathcal{Y}_Q^\dagger)^k$ to produce $\mathcal{S}((\mathcal{Y}_Q^\dagger)^k)$.

134 The main contributions of this paper can be summarized as follows.

- 135 • We prove that, under mild assumptions on sampling schemes, as $k \rightarrow +\infty$, every limit point
 136 in $\mathcal{S}((\mathcal{Y}_Q^\dagger)^k)$ is a point in $\mathcal{S}(\mathcal{Y}_Q^\dagger)$. That is, every point in $\mathcal{S}((\mathcal{Y}_Q^\dagger)^k)$ obtained from numerically
 137 solving the embedding problem with sufficiently large k can be an accurate approximation to
 138 an MV scalarization optimal point.
- 139 • The above result and the results developed in [27] form a numerical framework for determin-
 140 ing valid (i.e. not spurious) points on the original efficient frontier. As such, these results
 141 complement the theoretical results of the embedding technique developed in [21, 33] for multi-
 142 period or continuous time MV optimization. Note that we do not require convexity of the
 143 original problem.
- 144 • We illustrate the theoretical findings of this paper for an MV asset-liability problem under
 145 jump diffusions. In this case, the frontier generated by the embedding technique *does* contain
 146 spurious points. This example highlights the importance of our post-processing numerical
 147 method.

148 To focus on the main issue of embedding parameter discretization, we assume that each point in
 149 \mathcal{Y}_Q^\dagger is the exact solution of an embedded optimization problem corresponding to an embedding
 150 parameter.

151 The remainder of this paper is organized as follows. In Section 2, we summarize relevant major
 152 findings in [27] for removing spurious points which are used in subsequent sections of the paper. The

153 main theoretical results on asymptotic convergence of the computed MV embedded post-processed
154 set $\mathcal{S}((\mathcal{Y}_Q^\dagger)^k)$ are presented in Section 3. In Section 4, we provide a numerical example for the
155 MV asset-liability management under jump diffusions. This requires solution of an HJB partial
156 integro-differential equation (PIDE). In Section 5 we discuss application of our main results to
157 other techniques (such as a Monte Carlo, Backward Stochastic Differential Equation formulation)
158 for numerically solving the embedded control problem. Section 6 concludes the paper and outlines
159 possible future work.

160 2 Removal of spurious points by identifying SOPs

161 We first briefly summarize the main results in [27], following notation used in [27]. We denote by
162 $X(t)$ the underlying multi-dimensional stochastic process and by x a state of the stochastic system.
163 We use $c(\cdot)$ to denote the control, representing a strategy, as a function of the current state, i.e.
164 $c(\cdot) : (X(t), t) \mapsto c = c(X(t), t)$. Furthermore, we denote by W_t the total wealth at time t . Let
165 $E_{c(\cdot)}^{x,t}[W_T]$ and $Var_{c(\cdot)}^{x,t}[W_T]$ respectively denote the expectation and the variance of the terminal
166 wealth W_T conditional on the initial state (x, t) and on the control $c(\cdot)$.

167 2.1 MV Pareto optimal set

168 Since we are mainly interested in identifying spurious points on an efficient frontier, we analyze
169 MV optimality in terms of time T achievable expected value and variance of the wealth. We first
170 introduce a few definitions.

171 **Definition 2.1.** Let $(x_0, 0) = (X(t=0), t=0)$ denote the initial state. Let

$$172 \mathcal{Y} = \{ (Var_{c(\cdot)}^{x_0,0}[W_T], E_{c(\cdot)}^{x_0,0}[W_T]) : c(\cdot) \text{ admissible} \} \quad (2.1)$$

172 denote the **achievable MV objective set** and $\bar{\mathcal{Y}}$ denote its closure.

173 **Definition 2.2.** A point $(\mathcal{V}_*, \mathcal{E}_*) \in \bar{\mathcal{Y}}$ is a **Pareto (optimal) point** if there exists no admissible
174 strategy $c(\cdot)$ such that

$$E_{c(\cdot)}^{x_0,0}[W_T] \geq \mathcal{E}_* \\ Var_{c(\cdot)}^{x_0,0}[W_T] \leq \mathcal{V}_* ,$$

175 and at least one of the inequalities in equation (2.2) is strict. We denote by \mathcal{P} the set of Pareto
176 (optimal) points. Note that $\mathcal{P} \subseteq \bar{\mathcal{Y}}$.

177 Although the above definitions are intuitive, determining the points in \mathcal{P} requires solving a
178 difficult multi-objective optimization problem, which includes two conflicting criteria. A standard
179 scalarization method can be used to combine the two criteria into an optimization problem with a
180 single objective. More specifically, for an arbitrary scalar $\mu > 0$, we first define $\mathcal{Y}_{P(\mu)}$ to be the set
181 of scalarization optimal points for the parameter μ ,

$$182 \mathcal{Y}_{P(\mu)} = \{ (\mathcal{V}_*, \mathcal{E}_*) \in \bar{\mathcal{Y}} : \mu \mathcal{V}_* - \mathcal{E}_* = \inf_{(\mathcal{V}, \mathcal{E}) \in \mathcal{Y}} (\mu \mathcal{V} - \mathcal{E}) \} . \quad (2.2)$$

182 We then define the **MV scalarization optimal set**, denoted by \mathcal{Y}_P , as

$$\mathcal{Y}_P = \bigcup_{\mu > 0} \mathcal{Y}_{P(\mu)} . \quad (2.3)$$

183 where we note that it is possible for $\mathcal{Y}_{P(\mu)}$ to be empty for some $\mu > 0$.

184 We recognize the difference between the set of all MV Pareto optimal points \mathcal{P} and the set of
 185 MV scalarization optimal points \mathcal{Y}_P defined in equation (2.3). In general, $\mathcal{Y}_P \subseteq \mathcal{P}$. However, the
 186 converse may not hold, if the achievable MV objective set \mathcal{Y} is not convex. As in [27], we restrict
 187 our attention to determining \mathcal{Y}_P .

188 2.2 Embedding methods

189 As noted in [21, 33], the presence of the variance term in equation (2.2) causes difficulty, if we
 190 attempt to determine $\mathcal{Y}_{P(\mu)}$ by directly solving for the associated value function using dynamic
 191 programming. To overcome this difficulty, we can make use of the main result in [21, 33] concerning
 192 the embedding technique. Similar to \mathcal{Y}_P , we can describe embedding optimality in terms of an
 193 achievable objective point $(\mathcal{V}, \mathcal{E}) \in \mathcal{Y}$.

194 **Definition 2.3** (Embedded MV objective set). *The **embedded MV objective set** \mathcal{Y}_Q is defined*
 195 *by*

$$\mathcal{Y}_Q = \bigcup_{-\infty < \gamma < +\infty} \mathcal{Y}_{Q(\gamma)}. \quad (2.4)$$

196 *where*

$$\mathcal{Y}_{Q(\gamma)} = \{(\mathcal{V}_*, \mathcal{E}_*) \in \bar{\mathcal{Y}} : \mathcal{V}_* + \mathcal{E}_*^2 - \gamma \mathcal{E}_* = \inf_{(\mathcal{V}, \mathcal{E}) \in \mathcal{Y}} \mathcal{V} + \mathcal{E}^2 - \gamma \mathcal{E}\}. \quad (2.5)$$

197 **Remark 2.1** (Nonemptiness of $\mathcal{Y}_{Q(\gamma)}$). *Write $\mathcal{V} + \mathcal{E}^2 - \gamma \mathcal{E}$ as $\mathcal{V} + (\mathcal{E} - \gamma/2)^2 - \gamma^2/4$. Noting that*
 198 *variance $\mathcal{V} \geq 0$, we have that $\mathcal{V} + \mathcal{E}^2 - \gamma \mathcal{E}$ is bounded from below for any γ . If $\mathcal{Y} \neq \emptyset$, then $\mathcal{Y}_{Q(\gamma)} \neq \emptyset$*
 199 *$\forall \gamma$. Thus $\inf_{(\mathcal{V}, \mathcal{E}) \in \mathcal{Y}} \mathcal{V} + \mathcal{E}^2 - \gamma \mathcal{E}$ exists and the closure $\bar{\mathcal{Y}}$ contains $(\mathcal{V}_*, \mathcal{E}_*)$.*

200 **Remark 2.2** (Dynamic programming form). *Since*

$$\mathcal{V} + \mathcal{E}^2 - \gamma \mathcal{E} = E_{c(\cdot)}^{x_0, 0}[W_T^2] - (E_{c(\cdot)}^{x_0, 0}[W_T])^2 + (E_{c(\cdot)}^{x_0, 0}[W_T])^2 - \gamma E_{c(\cdot)}^{x_0, 0}[W_T] \quad (2.6)$$

$$= E_{c(\cdot)}^{x_0, 0}[W_T^2 - \gamma W_T] \quad (2.7)$$

201 *then we can write equation (2.5) in standard control form*

$$\inf_{(\mathcal{V}, \mathcal{E}) \in \mathcal{Y}} \mathcal{V} + \mathcal{E}^2 - \gamma \mathcal{E} = \inf_{c(\cdot)} E_{c(\cdot)}^{x_0, 0}[W_T^2 - \gamma W_T] \quad (2.8)$$

202 *which is now amenable to solution by a dynamic programming technique.*

203 **Definition 2.4.** *A point $(\mathcal{V}, \mathcal{E}) \in \mathcal{Y}_Q$ is a **spurious point** if $(\mathcal{V}, \mathcal{E}) \notin \mathcal{Y}_P$.*

204 We also introduce the concept of scalarization optimal points (SOPs) with respect to a set.

205 **Definition 2.5.** *Let \mathcal{X} be a non-empty subset of $\bar{\mathcal{Y}}$. We define*

$$\mathcal{S}_\mu(\mathcal{X}) = \{(\mathcal{V}_*, \mathcal{E}_*) \in \bar{\mathcal{X}} : \mu \mathcal{V}_* - \mathcal{E}_* = \inf_{(\mathcal{V}, \mathcal{E}) \in \mathcal{X}} \mu \mathcal{V} - \mathcal{E}\}, \quad (2.9)$$

206 *where $\bar{\mathcal{X}}$ is the closure of \mathcal{X} . We call a point in $\mathcal{S}_\mu(\mathcal{X})$ a **scalarization optimal point (SOP)** w.r.t.*
 207 *(\mathcal{X}, μ) . We also define*

$$\mathcal{S}(\mathcal{X}) = \{(\mathcal{V}_*, \mathcal{E}_*) : (\mathcal{V}_*, \mathcal{E}_*) \text{ is an SOP w.r.t. } (\mathcal{X}, \mu) \text{ for some } \mu > 0\}. \quad (2.10)$$

208 *We refer to $(\mathcal{V}_0, \mathcal{E}_0) \in \mathcal{S}(\mathcal{X})$ as **SOP w.r.t. \mathcal{X}** .*

209 Geometrically speaking, an SOP with respect to a set is a point at which there exists a sup-
 210 porting hyperplane with a positive slope for that set. We make the following assumption on the
 211 achievable objective set \mathcal{Y} .

212 **Assumption 2.1** (Nonemptiness). *We assume that \mathcal{Y} is a non-empty subset of $\{(\mathcal{V}, \mathcal{E}) \in \mathbf{R}^2 :$
 213 $\mathcal{V} \geq 0\}$ and that there exists a positive scalarization parameter $\mu_E > 0$ such that $\mathcal{S}_{\mu_E}(\mathcal{Y}) \neq \emptyset$.*

214 **Lemma 2.1** (Nonemptiness of $\mathcal{S}_\mu(\mathcal{Y}), \mu \geq \mu_E$). *If Assumption 2.1 holds, then $\forall \mu \geq \mu_E, \mathcal{S}_\mu(\mathcal{Y}) \neq$
 215 \emptyset .*

216 *Proof.* Let $(\mathcal{V}_E, \mathcal{E}_E) \in \mathcal{S}_{\mu_E}(\mathcal{Y})$. For any given $\mu \geq \mu_E$, consider $\forall (\mathcal{V}, \mathcal{E}) \in \mathcal{Y}$,

$$\mu\mathcal{V} - \mathcal{E} \geq \mu_E\mathcal{V} - \mathcal{E} \geq \mu_E\mathcal{V}_E - \mathcal{E}_E. \quad (2.11)$$

217 Hence, $\mathcal{S}_\mu(\mathcal{Y}) \neq \emptyset$ for all $\mu \geq \mu_E$. □

218 **Remark 2.3.** *Note that $\mathcal{V} \geq 0$ always holds since the variance is non-negative. In [27], to ensure
 219 that $\mathcal{Y}_{P(\mu)} \neq \emptyset$, a stronger assumption was made that $\forall (\mathcal{V}, \mathcal{E}) \in \mathcal{Y}, \mathcal{E} \leq C_E$, where C_E is a constant.
 220 Due to Lemma 2.1, the results in [27] hold under Assumption 2.1.*

221 The embedding result of [21, 33] is summarized in Theorem 2.1, under the weaker Assumption
 222 2.1. An important implication of Theorem 2.1 is that $\mathcal{Y}_P \subseteq \mathcal{Y}_Q$.

223 **Theorem 2.1** (Embedding result – Theorem 4.4 in [27]). *If Assumption 2.1 holds and $\mu \geq \mu_E$,
 224 then $\mathcal{S}_\mu(\mathcal{Y}) \neq \emptyset$. Assume $(\mathcal{V}_0, \mathcal{E}_0) \in \mathcal{Y}_{P(\mu)}$. Then*

$$\mu\mathcal{V}_0 - \mathcal{E}_0 = \inf_{(\mathcal{V}, \mathcal{E}) \in \mathcal{Y}} \mu\mathcal{V} - \mathcal{E} \quad (2.12)$$

225 and

$$\mathcal{V}_0 + \mathcal{E}_0^2 - \gamma\mathcal{E}_0 = \inf_{(\mathcal{V}, \mathcal{E}) \in \mathcal{Y}} \mathcal{V} + \mathcal{E}^2 - \gamma\mathcal{E}, \quad \text{i.e. } (\mathcal{V}_0, \mathcal{E}_0) \in \mathcal{Y}_{Q(\gamma)}, \quad (2.13)$$

226 where

$$\gamma = \frac{1}{\mu} + 2\mathcal{E}_0. \quad (2.14)$$

227 For subsequent analysis, we present the following uniqueness property of the embedded MV
 228 objective set $\mathcal{Y}_{Q(\gamma)}$ established in [27].

229 **Theorem 2.2** (Uniqueness of $\mathcal{Y}_{Q(\gamma)}$ – Theorem 4.8 in [27]). *If $(\mathcal{V}, \mathcal{E}) \in \mathcal{S}(\mathcal{Y}_Q)$, then there exists γ
 230 such that $(\mathcal{V}, \mathcal{E}) \in \mathcal{Y}_{Q(\gamma)}$ and $\mathcal{Y}_{Q(\gamma)}$ is a singleton.*

231 The following result from [27] indicates that spurious points can be identified as not being SOP
 232 with respect to the embedded MV objective set.

233 **Theorem 2.3** (Theorem 4.7 in [27]). *The SOPs w.r.t. \mathcal{Y}_Q are the same as the SOPs w.r.t. \mathcal{Y} , i.e.*

$$\mathcal{S}(\mathcal{Y}_Q) = \mathcal{Y}_P = \mathcal{S}(\mathcal{Y}). \quad (2.15)$$

234 Theorem 2.3 demonstrates that it is possible to generate the original MV SOP set \mathcal{Y}_P from the
 235 embedded MV objective set \mathcal{Y}_Q . More specifically, a spurious point in \mathcal{Y}_Q is a point at which there
 236 does not exist a supporting hyperplane with positive slope for \mathcal{Y}_Q . Excluding all these spurious
 237 points from \mathcal{Y}_Q , we obtain $\mathcal{S}(\mathcal{Y}_Q)$, and hence, \mathcal{Y}_P .

238 **Remark 2.4** (Existence of Spurious Points). *Spurious points can arise from two distinct causes.*
239 *If the original MV problem is not convex, then it is easily seen that spurious points can be gener-*
240 *ated. However, even if the MV problem is convex, a numerical algorithm based on minimizing the*
241 *objective function (2.5) may produce spurious points (as defined in Definition 2.4). This is because*
242 *numerically computed points in \mathcal{Y}_Q may not satisfy all the conditions (2.12)–(2.14). If we have a*
243 *closed form solution, as in [21, 33], then necessary condition (2.14) (where μ satisfies (2.12)) can*
244 *be explicitly imposed, so that this situation does not arise. However, given an arbitrary point in*
245 *\mathcal{Y}_Q , generated by a numerical algorithm, then we cannot verify that condition (2.14) is satisfied,*
246 *without examining the entire set \mathcal{Y}_Q . However, we can ensure that both types of spurious points can*
247 *be eliminated if we consider only the S.O.Ps w.r.t \mathcal{Y}_Q as in Theorem 2.3. Note that spurious points*
248 *were not generated in [21, 33], since the MV problems considered were convex, and the closed-form*
249 *solutions enabled imposition of condition (2.14).*

250 **2.3 Removal of spurious points with respect to the computed embedded MV** 251 **set**

252 However, Theorem 2.3 cannot be directly used in a numerical algorithm for construction of $\mathcal{S}(\mathcal{Y}_Q)$,
253 since the entire set \mathcal{Y}_Q is not available in practice. There are two aspects of incompleteness. The
254 first is the incompleteness due to availability of only a single solution for each γ . For each embedding
255 parameter γ , $-\infty < \gamma < +\infty$, a numerical algorithm applied to the embedded problem can generate
256 only a single embedded MV point $(\mathcal{V}, \mathcal{E}) \in \mathcal{Y}_{Q(\gamma)}$. In this case, it is not obvious that the single
257 embedded MV point generated by our algorithm will satisfy all the conditions (2.12)–(2.14). This
258 first aspect of incompleteness is addressed in [27]; the relevant result is summarized below. The
259 second aspect of incompleteness is due to the fact that, in practice, only a finite number of γ values
260 can be used to approximate the set \mathcal{Y}_Q . This aspect of incompleteness is the focus of this paper,
261 and is discussed in Section 3. We define the **computed MV embedded objective set**, denoted
262 by \mathcal{Y}_Q^\dagger , as follows.

263 **Definition 2.6** (Computed MV embedded objective set). *Let $\mathcal{Y}_{Q(\gamma)}^\dagger$ be a singleton subset of $\mathcal{Y}_{Q(\gamma)}$.*
264 *Specifically $\mathcal{Y}_{Q(\gamma)}^\dagger$ contains either*

- 265 • *the unique single point which is SOP w.r.t. \mathcal{Y}_Q if $\mathcal{Y}_{Q(\gamma)}$ is the singleton set containing a point*
266 *SOP w.r.t. \mathcal{Y}_Q , or*
- 267 • *an arbitrarily selected single point of $\mathcal{Y}_{Q(\gamma)}$ otherwise.*

268 *The computed MV objective set is then defined as*

$$\mathcal{Y}_Q^\dagger = \bigcup_{-\infty < \gamma < +\infty} \mathcal{Y}_{Q(\gamma)}^\dagger.$$

269 The following theorem shows that \mathcal{Y}_P can be generated from \mathcal{Y}_Q^\dagger .

270 **Theorem 2.4** (Theorem 5.4 in [27]). *Suppose Assumption 2.1 holds. Then*

$$\mathcal{S}(\mathcal{Y}_Q^\dagger) = \mathcal{Y}_P = \mathcal{S}(\mathcal{Y}) . \tag{2.16}$$

271 Following immediately from Theorem 2.4, Lemma 2.1, we have Corollary 2.1.

272 **Corollary 2.1.** *Suppose Assumption 2.1 holds. Then $\mathcal{S}_\mu(\mathcal{Y}_Q^\dagger) \neq \emptyset, \forall \mu \geq \mu_E$.*

273 An important implication of Theorem 2.4 is that, given an MV point $(\mathcal{V}, \mathcal{E}) \in \mathcal{Y}_Q^\dagger$, we can
 274 determine whether it is in \mathcal{Y}_P by checking whether it is an SOP with respect to \mathcal{Y}_Q^\dagger .

275 3 Asymptotic properties of sets of SOPs with respect to the em- 276 bedding parameter sampling

277 It is important to note that the procedure given in [27], described so far, requires the entire set
 278 \mathcal{Y}_Q^\dagger to be available, i.e. an embedded MV point for each $\gamma \in (-\infty, +\infty)$. However, we typically
 279 solve the embedded problem for each fixed γ by numerically solving the associated HJB equation.
 280 Hence, in practice, we can only approximate \mathcal{Y}_Q^\dagger for a finite number of γ values. More specifically,
 281 we approximate \mathcal{Y}_Q^\dagger using a finite set of γ values, each of which yields a solution to the embedded
 282 problem (2.13). As a result, a sampling discretization for γ needs to be implemented. In addition, to
 283 assess convergence of the approximation of \mathcal{Y}_Q^\dagger , a sequence of samplings of γ needs to be computed.
 284 To capture this, we denote by Γ_k the finite discrete set of sampled γ values at the sampling
 285 discretization level k . Examples of methods for constructing Γ_k are given in §3.2. Let

$$(\mathcal{Y}_Q^\dagger)^k = \bigcup_{\gamma \in \Gamma_k} \mathcal{Y}_{Q(\gamma)}^\dagger \quad (3.1)$$

286 denote the set of all computed MV embedded points using the sampling set Γ^k . Note that

$$(\mathcal{Y}_Q^\dagger)^k \subseteq \mathcal{Y}_Q^\dagger. \quad (3.2)$$

287 In addition, we need to construct the SOPs of $(\mathcal{Y}_Q^\dagger)^k$, i.e. $\mathcal{S}((\mathcal{Y}_Q^\dagger)^k)$. A simple method which
 constructs $\mathcal{S}((\mathcal{Y}_Q^\dagger)^k)$ is described in Algorithm 3.1. Theoretical justification of Algorithm 3.1 is

Algorithm 3.1 Post-processing algorithm to construct $\mathcal{S}((\mathcal{Y}_Q^\dagger)^k)$ from $(\mathcal{Y}_Q^\dagger)^k$.

- 1: determine the set $(\mathcal{C})^k$ consisting of all the vertices of the convex hull of $(\mathcal{Y}_Q^\dagger)^k$;
 - 2: determine the set $(\mathcal{U})^k$ consisting of upper-left boundary points of $(\mathcal{C})^k$;
 - 3: return $\mathcal{S}((\mathcal{Y}_Q^\dagger)^k) \equiv (\mathcal{U})^k$.
-

288 given in [27]. In [27], it is conjectured that for sufficiently large k , the points in $\mathcal{S}((\mathcal{Y}_Q^\dagger)^k)$ sufficiently
 289 well approximate the points in $\mathcal{S}((\mathcal{Y}_Q^\dagger)) = \mathcal{Y}_P$. In this section, we analyze convergence properties
 290 of $(\mathcal{Y}_Q^\dagger)^k$ as $k \rightarrow +\infty$. Our aim is to show that, as $k \rightarrow +\infty$, every limit point of a sequence
 291 $\{(\mathcal{E}_k, \mathcal{V}_k)\}$, $(\mathcal{E}_k, \mathcal{V}_k) \in \mathcal{S}_\mu((\mathcal{Y}_Q^\dagger)^k)$, is a point in $\mathcal{S}_\mu(\mathcal{Y}_Q^\dagger)$.

293 **Remark 3.1** (Intuitive explanation of Algorithm 3.1). *Note that $(\mathcal{Y}_Q^\dagger)^k$ is a finite set of points. If
 294 a point is in $\mathcal{S}((\mathcal{Y}_Q^\dagger)^k)$, then there exists a supporting hyperplane with positive slope at that point.
 295 These points are also the vertices of the upper left convex hull of $(\mathcal{Y}_Q^\dagger)^k$ [27]. The vertices of the
 296 upper left convex hull of m points can be computed in $O(m \log m)$ time, using, for example, the
 297 algorithm in [2].*

298 **3.1 Preliminaries**

299 In preparation for the convergence analysis, we first establish a few technical lemmas. Recall that

$$\mathcal{S}_\mu(\mathcal{Y}_Q^\dagger) = \{(\mathcal{V}_*, \mathcal{E}_*) \in \overline{\mathcal{Y}_Q^\dagger} : \mu\mathcal{V}_* - \mathcal{E}_* = \inf_{(\mathcal{V}, \mathcal{E}) \in \mathcal{Y}_Q^\dagger} \mu\mathcal{V} - \mathcal{E}\}. \quad (3.3)$$

300 One thing that makes the asymptotic analysis challenging is that, for a given μ , there can be
 301 multiple points in $\mathcal{S}_\mu(\mathcal{Y}_Q^\dagger)$. We handle this difficulty by examining the minimum element of $\mathcal{S}_\mu(\mathcal{Y}_Q^\dagger)$
 302 for each given μ .

303 **Definition 3.1.** For $\mathcal{S}_\mu(\mathcal{Y}_Q^\dagger) \neq \emptyset$, $\mu > 0$, we define the minimum element as $(\mathcal{V}^{\min}(\mu), \mathcal{E}^{\min}(\mu))$
 304 where

$$(\mathcal{V}^{\min}(\mu), \mathcal{E}^{\min}(\mu)) \in \mathcal{S}_\mu(\mathcal{Y}_Q^\dagger), \quad \mathcal{V}^{\min}(\mu) \leq \mathcal{V}, \quad \mathcal{E}^{\min}(\mu) \leq \mathcal{E}, \quad \forall (\mathcal{V}, \mathcal{E}) \in \mathcal{S}_\mu(\mathcal{Y}_Q^\dagger). \quad (3.4)$$

305 **3.1.1 Minimum element of $\mathcal{S}_\mu(\mathcal{Y}_Q^\dagger)$**

306 Since any point in $\mathcal{S}_\mu(\mathcal{Y}_Q^\dagger)$ lies on a supporting hyperplane with a slope $\mu > 0$, we immediately have
 307 the following Lemma concerning the existence and uniqueness of the minimum element of $\mathcal{S}_\mu(\mathcal{Y}_Q^\dagger)$.

308 **Lemma 3.1.** Assume that $\mathcal{S}_\mu(\mathcal{Y}_Q^\dagger) \neq \emptyset$ for $\mu > 0$. Then there exists a unique minimum
 309 $(\mathcal{V}^{\min}(\mu), \mathcal{E}^{\min}(\mu))$ for $\mathcal{S}_\mu(\mathcal{Y}_Q^\dagger)$. In addition,

$$\begin{aligned} \mathcal{V}^{\min}(\mu) &= \inf_{(\mathcal{V}, \mathcal{E}) \in \mathcal{S}_\mu(\mathcal{Y}_Q^\dagger)} \mathcal{V}, \\ \mathcal{E}^{\min}(\mu) &= \mu\mathcal{V}^{\min}(\mu) - \inf_{(\mathcal{V}, \mathcal{E}) \in \mathcal{Y}_Q^\dagger} \mu\mathcal{V} - \mathcal{E}. \end{aligned}$$

310 *Proof.* Let $\mu > 0$ be given. Since $\mathcal{S}_\mu(\mathcal{Y}_Q^\dagger) \neq \emptyset$, there exists the unique value

$$f_0(\mu) = \inf_{(\mathcal{V}, \mathcal{E}) \in \mathcal{Y}_Q^\dagger} \mu\mathcal{V} - \mathcal{E}. \quad (3.5)$$

311 Then,

$$\mu\mathcal{V} - \mathcal{E} = f_0(\mu), \quad \forall (\mathcal{V}, \mathcal{E}) \in \mathcal{S}_\mu(\mathcal{Y}_Q^\dagger). \quad (3.6)$$

312 To show existence and uniqueness of $\mathcal{V}^{\min}(\mu)$, we note that $\mathcal{V} \geq 0$, i.e. \mathcal{V} is bounded below.
 313 Hence, $\inf_{(\mathcal{V}, \mathcal{E}) \in \mathcal{S}_\mu(\mathcal{Y}_Q^\dagger)} \mathcal{V}$ exists. Let

$$\mathcal{V}^{\min}(\mu) = \inf_{(\mathcal{V}, \mathcal{E}) \in \mathcal{S}_\mu(\mathcal{Y}_Q^\dagger)} \mathcal{V}. \quad (3.7)$$

314 Clearly, $\mathcal{V}^{\min}(\mu)$ is unique. In addition, we have

$$\mathcal{V}^{\min}(\mu) \leq \mathcal{V}, \quad \forall (\mathcal{V}, \mathcal{E}) \in \mathcal{S}_\mu(\mathcal{Y}_Q^\dagger).$$

315 Now, we show existence and uniqueness of quantity $\mathcal{E}^{\min}(\mu)$. To this end, note that, there exists
 316 a sequence $\{(\mathcal{V}_k, \mathcal{E}_k)\}$, $(\mathcal{V}_k, \mathcal{E}_k) \in \mathcal{S}_\mu(\mathcal{Y}_Q^\dagger)$, such that

$$\lim_{k \rightarrow +\infty} \mathcal{V}_k = \mathcal{V}^{\min}(\mu).$$

317 For any sequence $\{(\mathcal{V}_k, \mathcal{E}_k)\}$, $(\mathcal{V}_k, \mathcal{E}_k) \in \mathcal{S}_\mu(\mathcal{Y}_Q^\dagger)$, with $\lim_{k \rightarrow +\infty} \mathcal{V}_k = \mathcal{V}^{\min}(\mu)$, we have

$$\mu \mathcal{V}_k - \mathcal{E}_k = f_0(\mu).$$

318 Thus,

$$\lim_{k \rightarrow +\infty} \mathcal{E}_k = \lim_{k \rightarrow +\infty} (\mu \mathcal{V}_k) - f_0(\mu) = \mu \mathcal{V}^{\min}(\mu) - f_0(\mu).$$

319 Define the unique value

$$\mathcal{E}^{\min}(\mu) = \lim_{k \rightarrow +\infty} \mathcal{E}_k = \mu \mathcal{V}^{\min}(\mu) - f_0(\mu), \quad (3.8)$$

320 or equivalently,

$$\mu \mathcal{V}^{\min}(\mu) - \mathcal{E}^{\min}(\mu) = f_0(\mu). \quad (3.9)$$

321 By (3.3), (3.5) and (3.9), it follows that $(\mathcal{V}^{\min}(\mu), \mathcal{E}^{\min}(\mu)) \in \mathcal{S}_\mu(\mathcal{Y}_Q^\dagger)$. From (3.6) and (3.9), we
 322 have

$$\mathcal{E}^{\min}(\mu) = \mu \mathcal{V}^{\min}(\mu) - (\mu \mathcal{V} - \mathcal{E}) \quad , \quad \forall (\mathcal{V}, \mathcal{E}) \in \mathcal{S}_\mu(\mathcal{Y}_Q^\dagger).$$

323 Hence, Lemma 3.1 holds. □

324 3.1.2 Continuity of $(\mathcal{V}^{\min}(\mu), \mathcal{E}^{\min}(\mu))$

325 Now we show that $(\mathcal{V}^{\min}(\mu), \mathcal{E}^{\min}(\mu))$ is right-continuous in μ . In the following supporting Lemma,
 326 we first establish the monotonicity of $(\mathcal{V}^{\min}(\mu), \mathcal{E}^{\min}(\mu))$.

327 **Lemma 3.2.** *Assume $\mathcal{S}_\mu(\mathcal{Y}_Q^\dagger) \neq \emptyset$. Let $(\mathcal{V}^{\min}(\mu), \mathcal{E}^{\min}(\mu)) \in \mathcal{S}_\mu(\mathcal{Y}_Q^\dagger)$, and $(\mathcal{V}^{\min}(\mu'), \mathcal{E}^{\min}(\mu')) \in$
 328 $\mathcal{S}_{\mu'}(\mathcal{Y}_Q^\dagger)$. If $\mu' > \mu$, then*

$$\mathcal{V}^{\min}(\mu') \leq \mathcal{V}^{\min}(\mu) \quad \text{and} \quad \mathcal{E}^{\min}(\mu') \leq \mathcal{E}^{\min}(\mu). \quad (3.10)$$

329 *Proof.* From Corollary 2.1, $\mathcal{S}_{\mu'}(\mathcal{Y}_Q^\dagger) \neq \emptyset$. Since $(\mathcal{V}^{\min}(\mu'), \mathcal{E}^{\min}(\mu')) \in \mathcal{S}_{\mu'}(\mathcal{Y}_Q^\dagger) \subseteq \overline{\mathcal{Y}_Q^\dagger}$, there exists a
 330 sequence $\{(\mathcal{V}_k, \mathcal{E}_k)\}$, $(\mathcal{V}_k, \mathcal{E}_k) \in \mathcal{Y}_Q^\dagger$, such that

$$\lim_{k \rightarrow \infty} \mathcal{V}_k = \mathcal{V}^{\min}(\mu') \quad \text{and} \quad \lim_{k \rightarrow \infty} \mathcal{E}_k = \mathcal{E}^{\min}(\mu'). \quad (3.11)$$

331 Since $(\mathcal{V}^{\min}(\mu), \mathcal{E}^{\min}(\mu)) \in \mathcal{S}_\mu(\mathcal{Y}_Q^\dagger)$,

$$\mu \mathcal{V}^{\min}(\mu) - \mathcal{E}^{\min}(\mu) \leq \mu \mathcal{V} - \mathcal{E}, \quad \forall (\mathcal{V}, \mathcal{E}) \in \mathcal{Y}_Q^\dagger. \quad (3.12)$$

332 From (3.11) and (3.12), we have

$$\mu \mathcal{V}^{\min}(\mu) - \mathcal{E}^{\min}(\mu) \leq \mu \mathcal{V}^{\min}(\mu') - \mathcal{E}^{\min}(\mu'). \quad (3.13)$$

333 Interchanging the role of μ and μ' in (3.13), we have

$$-(\mu'\mathcal{V}^{\min}(\mu) - \mathcal{E}^{\min}(\mu)) \leq -(\mu'\mathcal{V}^{\min}(\mu') - \mathcal{E}^{\min}(\mu')). \quad (3.14)$$

334 Adding (3.13) and (3.14) gives

$$(\mu - \mu')\mathcal{V}^{\min}(\mu) \leq (\mu - \mu')\mathcal{V}^{\min}(\mu') \Rightarrow (\mu - \mu')(\mathcal{V}^{\min}(\mu) - \mathcal{V}^{\min}(\mu')) \leq 0. \quad (3.15)$$

335 Since $\mu' > \mu$, it follows from (3.15) that $\mathcal{V}^{\min}(\mu') \leq \mathcal{V}^{\min}(\mu)$.

336 By first multiplying (3.13) and (3.14) with μ' and μ , respectively, then adding the resulting
337 inequalities, we obtain

$$(\mu - \mu')(\mathcal{E}^{\min}(\mu) - \mathcal{E}^{\min}(\mu')) \leq 0.$$

338 It follows that $\mathcal{E}^{\min}(\mu') \leq \mathcal{E}^{\min}(\mu)$. □

339 Next we establish that $(\mathcal{V}^{\min}(\mu), \mathcal{E}^{\min}(\mu)) \in \mathcal{S}_\mu(\mathcal{Y}_Q^\dagger)$ is right-continuous in μ .

340 **Lemma 3.3.** *Assume that $\mathcal{S}_\mu(\mathcal{Y}_Q^\dagger) \neq \emptyset$ at $\mu = \mu_0$. Then, $(\mathcal{V}^{\min}(\mu), \mathcal{E}^{\min}(\mu)) \in \mathcal{S}_\mu(\mathcal{Y}_Q^\dagger)$ are right-
341 continuous in $[\mu_0, +\infty)$.*

342 *Proof.* From Corollary 2.1, $\mathcal{S}_\mu(\mathcal{Y}_Q^\dagger) \neq \emptyset$ for all $\mu \geq \mu_0$. Let $(\mathcal{V}^{\min}(\mu), \mathcal{E}^{\min}(\mu)) \in \mathcal{S}_\mu(\mathcal{Y}_Q^\dagger)$, and
343 $(\mathcal{V}^{\min}(\mu_0), \mathcal{E}^{\min}(\mu_0)) \in \mathcal{S}_{\mu_0}(\mathcal{Y}_Q^\dagger)$. Following Lemma 3.2, we have

$$\mathcal{E}^{\min}(\mu) \leq \mathcal{E}^{\min}(\mu_0), \quad \text{and} \quad \mathcal{V}^{\min}(\mu) \leq \mathcal{V}^{\min}(\mu_0), \quad \forall \mu \geq \mu_0. \quad (3.16)$$

344 Due to this monotonicity, there exists $(\mathcal{E}_L, \mathcal{V}_L) \in \overline{\mathcal{Y}_Q^\dagger}$ such that

$$\lim_{\mu \rightarrow \mu_0^+} \mathcal{E}^{\min}(\mu) = \mathcal{E}_L, \quad \text{and} \quad \lim_{\mu \rightarrow \mu_0^+} \mathcal{V}^{\min}(\mu) = \mathcal{V}_L. \quad (3.17)$$

345 To show right-continuity, we now establish that $\mathcal{E}_L = \mathcal{E}^{\min}(\mu)$ and $\mathcal{V}_L = \mathcal{V}^{\min}(\mu)$. From (3.16)-
346 (3.17), we conclude that

$$\mathcal{E}_L \leq \mathcal{E}^{\min}(\mu_0); \quad \mathcal{V}_L \leq \mathcal{V}^{\min}(\mu_0). \quad (3.18)$$

347 Since

$$\mu\mathcal{V}^{\min}(\mu) - \mathcal{E}^{\min}(\mu) \leq \mu\mathcal{V} - \mathcal{E}, \quad \forall (\mathcal{V}, \mathcal{E}) \in \mathcal{Y}_Q^\dagger,$$

348 by letting $\mu \rightarrow \mu_0^+$ and using (3.17), we obtain

$$\mu_0\mathcal{V}_L - \mathcal{E}_L \leq \mu_0\mathcal{V} - \mathcal{E}, \quad \forall (\mathcal{V}, \mathcal{E}) \in \mathcal{Y}_Q^\dagger. \quad (3.19)$$

349 Since $(\mathcal{E}_L, \mathcal{V}_L) \in \overline{\mathcal{Y}_Q^\dagger}$, and $(\mathcal{V}^{\min}(\mu_0), \mathcal{E}^{\min}(\mu_0)) \in \mathcal{S}_{\mu_0}(\mathcal{Y}_Q^\dagger) \subseteq \mathcal{Y}_Q^\dagger$, it follows from (3.19) that

$$\mu_0\mathcal{V}_L - \mathcal{E}_L = \mu_0\mathcal{V}^{\min}(\mu_0) - \mathcal{E}^{\min}(\mu_0).$$

350 Hence, $(\mathcal{E}_L, \mathcal{V}_L) \in \mathcal{S}_{\mu_0}(\mathcal{Y}_Q^\dagger)$. By Lemma 3.1, we have

$$\mathcal{V}^{\min}(\mu_0) \leq \mathcal{V}_L, \quad \mathcal{E}^{\min}(\mu_0) \leq \mathcal{E}_L. \quad (3.20)$$

351 From (3.18) and (3.20), it follows that $\mathcal{E}_L = \mathcal{E}^{\min}(\mu)$ and $\mathcal{V}_L = \mathcal{V}^{\min}(\mu)$. □

352 **3.1.3 Continuity and monotonicity of $\gamma^{\min}(\mu)$**

353 We note that the embedding parameter $\gamma^{\min}(\mu)$, corresponding to the minimum element, also plays
 354 an important role in the asymptotic analysis. Next, we show that, assuming $(\mathcal{V}^{\min}(\mu), \mathcal{E}^{\min}(\mu))$
 355 exists, the corresponding embedding parameter $\gamma^{\min}(\mu)$ is right-continuous and strictly decreasing
 356 in μ . First, we establish a supporting Lemma that relates the embedding parameter γ^{\min} and the
 357 scalarization parameter μ .

358 **Lemma 3.4.** *Assume that $\mathcal{S}_\mu(\mathcal{Y}_Q^\dagger) \neq \emptyset$ and that $(\mathcal{V}^{\min}(\mu), \mathcal{E}^{\min}(\mu)) \in \mathcal{S}_\mu(\mathcal{Y}_Q^\dagger)$. Then, there exists
 359 a unique $\gamma^{\min}(\mu)$ such that*

$$\begin{aligned} \gamma^{\min}(\mu) &= \frac{1}{\mu} + 2\mathcal{E}^{\min}(\mu), \\ &\text{where } (\mathcal{V}^{\min}(\mu), \mathcal{E}^{\min}(\mu)) \in \mathcal{Y}_{Q(\gamma^{\min}(\mu))}^\dagger, \end{aligned} \quad (3.21)$$

360 and $(\mathcal{V}^{\min}(\mu), \mathcal{E}^{\min}(\mu))$ is the unique point in $\mathcal{Y}_{Q(\gamma^{\min}(\mu))}^\dagger \subseteq \mathcal{S}(\mathcal{Y}_Q^\dagger)$.

361 *Proof.* Since $(\mathcal{V}^{\min}(\mu), \mathcal{E}^{\min}(\mu)) \in \mathcal{S}_\mu(\mathcal{Y}_Q^\dagger) \subseteq \mathcal{S}(\mathcal{Y}_Q^\dagger)$, following Theorem 2.4, we have

$$(\mathcal{V}^{\min}(\mu), \mathcal{E}^{\min}(\mu)) \in \mathcal{Y}_P = \mathcal{S}(\mathcal{Y}).$$

362 By Theorem 2.3, we have $\mathcal{S}(\mathcal{Y}) = \mathcal{S}(\mathcal{Y}_Q)$. Hence

$$(\mathcal{V}^{\min}(\mu), \mathcal{E}^{\min}(\mu)) \in \mathcal{S}(\mathcal{Y}_Q).$$

363 Using Theorem 2.2, we have

$$(\mathcal{V}^{\min}(\mu), \mathcal{E}^{\min}(\mu)) \in \mathcal{Y}_{Q(\gamma)} \quad \text{for some } \gamma,$$

364 and $\mathcal{Y}_{Q(\gamma)}$ is a singleton. Following Theorem 2.1, there exists an unique $\gamma^{\min}(\mu)$, which is defined
 365 below

$$\gamma^{\min}(\mu) = \frac{1}{\mu} + 2\mathcal{E}^{\min}(\mu).$$

366 By Definition 2.6, $\mathcal{Y}_{Q(\gamma)}^\dagger$ contains a single point, so that $(\mathcal{V}^{\min}(\mu), \mathcal{E}^{\min}(\mu))$ is the unique point in
 367 $\mathcal{Y}_{Q(\gamma^{\min}(\mu))}^\dagger$. This completes the proof. \square

368 In the following Lemma, we establish the right-continuity and monotonicity of $\gamma^{\min}(\mu)$ in μ .

369 **Lemma 3.5.** *Assume that $\mathcal{S}_\mu(\mathcal{Y}_Q^\dagger) \neq \emptyset$ for $\mu = \mu_0 > 0$. Then $\gamma^{\min}(\mu)$ is right-continuous and
 370 strictly decreasing in $[\mu_0, +\infty)$.*

371 *Proof.* From Corollary 2.1, $\mathcal{S}_\mu(\mathcal{Y}_Q^\dagger) \neq \emptyset$ for any $\mu \in [\mu_0, +\infty)$, and from Lemma 3.3, $\mathcal{E}^{\min}(\mu)$
 372 is right-continuous in $[\mu_0, +\infty)$. Thus, from (3.21), $\gamma^{\min}(\mu)$ is right-continuous in μ . To show
 373 monotonicity, note that, for any $\mu, \mu' \in (\mu_0, +\infty)$ and $\mu > \mu'$, we have (noting Lemma 3.2)

$$\frac{1}{\mu} < \frac{1}{\mu'} \quad ; \quad \mathcal{E}^{\min}(\mu) \leq \mathcal{E}^{\min}(\mu'). \quad (3.22)$$

374 Thus, from (3.21)-(3.22), we have that $\gamma^{\min}(\mu)$ is a strictly decreasing function of μ in $[\mu_0, +\infty)$. \square

375 From Lemma 3.5, $\gamma^{\min}(\mu)$ is a strictly decreasing function of μ in $[\mu_0, +\infty)$. Following this,
 376 we immediately conclude that the inverse function $\gamma^{\min^{-1}}(\gamma)$, which yields an unique scalarization
 377 parameter, is left continuous at $\gamma^{\min}(\mu_0)$. Specifically, the inverse function $\gamma^{\min^{-1}}(\gamma)$ is uniquely
 378 defined in $(\underline{\gamma_0}^{\min}, \gamma^{\min}(\mu_0)]$ for some $\underline{\gamma_0}^{\min}$.

379 Next we analyze asymptotic properties of embedded MV points corresponding to a set Γ_k of
 380 sampled embedding parameter γ under some mild assumptions on Γ_k , see, e.g., Assumption 3.1.

381 **Lemma 3.6.** *Assume that $\mathcal{S}_\mu(\mathcal{Y}_Q^\dagger) \neq \emptyset$ at $\mu = \mu_0$. Let $(\mathcal{V}^{\min}(\mu_0), \mathcal{E}^{\min}(\mu_0)) \in \mathcal{S}_{\mu_0}(\mathcal{Y}_Q^\dagger)$. Assume
 382 that there exists a monotonically increasing sequence of embedding parameters $\{\gamma_k\}$ satisfying*

$$\lim_{k \rightarrow \infty} \gamma_k = \gamma^{\min}(\mu_0) \quad ; \quad \gamma_k \geq \gamma_{k-1} .$$

383 *Then for sufficiently large k , there exists a unique μ_k such that*

$$\mu_k = \gamma^{\min^{-1}}(\gamma_k), \quad \mu_k \geq \mu_0,$$

384 *and*

$$\lim_{k \rightarrow \infty} (\mathcal{V}^{\min}(\mu_k), \mathcal{E}^{\min}(\mu_k)) = (\mathcal{V}^{\min}(\mu_0), \mathcal{E}^{\min}(\mu_0)) .$$

385 *Proof.* Since $\mathcal{S}_\mu(\mathcal{Y}_Q^\dagger) \neq \emptyset$ at $\mu = \mu_0$, from Lemma 3.5, $\gamma^{\min}(\mu)$ is monotonically decreasing and
 386 right-continuous in $[\mu_0, +\infty)$. Hence, from Lemma 3.5, for sufficiently large k , there exists a unique
 387 μ_k such that

$$\mu_k = \gamma^{\min^{-1}}(\gamma_k), \quad \mu_k \geq \mu_0$$

388 and μ_k monotonically decreasing, such that

$$\lim_{k \rightarrow \infty} \mu_k = \mu_0$$

389 Note that $(\mathcal{V}^{\min}(\mu_0), \mathcal{E}^{\min}(\mu_0)) \in \mathcal{S}_{\mu_0}(\mathcal{Y}_Q^\dagger)$ is unique. In addition there exists unique

$$(\mathcal{V}^{\min}(\mu_k), \mathcal{E}^{\min}(\mu_k)) \in \mathcal{S}_{\mu_k}(\mathcal{Y}_Q^\dagger).$$

390 Furthermore,

$$\lim_{k \rightarrow \infty} (\mathcal{V}^{\min}(\mu_k), \mathcal{E}^{\min}(\mu_k)) = (\mathcal{V}^{\min}(\mu_0), \mathcal{E}^{\min}(\mu_0)),$$

391 which follows from the right-continuity of $(\mathcal{V}^{\min}(\mu_k), \mathcal{E}^{\min}(\mu_k))$ in $[\mu_0, +\infty)$. \square

392 We conclude this subsection with a lemma which can be used to identify possible spurious points
 393 by examining only a subinterval of values of the embedding parameter γ .

394 **Lemma 3.7.** *Let Assumption 2.1 hold. Assume that there exists \mathcal{E}^* such that*

$$\mathcal{E}^* = \liminf_{\mu \rightarrow +\infty} \{\mathcal{E}_\mu : (\mathcal{V}_\mu, \mathcal{E}_\mu) \in \mathcal{S}_\mu(\mathcal{Y})\} . \quad (3.23)$$

395 *Then for any $\hat{\mu} > \mu_E$, there exists $\hat{\gamma}$, $-\infty < \hat{\gamma} < \infty$, such that*

$$\hat{\gamma} = \frac{1}{\hat{\mu}} + 2\mathcal{E}^{\min}(\hat{\mu}). \quad (3.24)$$

where $(\mathcal{V}^{\min}(\hat{\mu}), \mathcal{E}^{\min}(\hat{\mu})) \in \mathcal{S}_{\hat{\mu}}(\mathcal{Y})$ and $(\mathcal{V}^{\min}(\hat{\mu}), \mathcal{E}^{\min}(\hat{\mu})) \in \mathcal{Y}_{Q(\hat{\gamma})}$. In addition

$$\hat{\gamma} > 2\mathcal{E}^* .$$

396 *Proof.* Since Assumption 2.1 holds, $\exists \mu_E > 0$ such that $\mathcal{S}_{\mu_E}(\mathcal{Y}) \neq \emptyset$. Hence $(\mathcal{V}^{\min}(\hat{\mu}), \mathcal{E}^{\min}(\hat{\mu})) \in$
 397 $\mathcal{S}_{\hat{\mu}}(\mathcal{Y})$ for $\hat{\mu} \geq \mu_E$. By Theorem 2.1, there exists $\hat{\gamma}$, $-\infty < \hat{\gamma} < \infty$, such that

$$\hat{\gamma} = \frac{1}{\hat{\mu}} + 2\mathcal{E}^{\min}(\hat{\mu}). \quad (3.25)$$

398 where $(\mathcal{V}^{\min}(\hat{\mu}), \mathcal{E}^{\min}(\hat{\mu})) \in \mathcal{Y}_{Q(\hat{\gamma})}$. From Lemma 3.2, $\mathcal{E}^{\min}(\hat{\mu})$ is non-increasing with respect to $\hat{\mu}$.
 399 Hence, from (3.23), we have that

$$\mathcal{E}^{\min}(\hat{\mu}) \geq \mathcal{E}^* .$$

400 Since $\hat{\mu} > 0$, from (3.24), we have $\hat{\gamma} > 2\mathcal{E}^{\min}(\hat{\mu}) \geq 2\mathcal{E}^*$. □

401 **Remark 3.2.** Lemma 3.7 has the following important implication. Suppose that $(\mathcal{V}^{\min}, \mathcal{E}^{\min})$ is
 402 an optimal MV point for some embedding parameter $\hat{\gamma}$, i.e., $(\mathcal{V}^{\min}, \mathcal{E}^{\min}) \in \mathcal{Y}_{Q(\hat{\gamma})}$. If $\hat{\gamma} < 2\mathcal{E}^*$ and
 403 there exists no $\tilde{\gamma}$ such that $\tilde{\gamma} > 2\mathcal{E}^*$ and $(\mathcal{V}^{\min}, \mathcal{E}^{\min}) \in \mathcal{Y}_{Q(\tilde{\gamma})}$, then $(\mathcal{V}^{\min}, \mathcal{E}^{\min})$ is a spurious point.

404 3.2 Asymptotic Convergence of $\mathcal{S}((\mathcal{Y}_Q^\dagger)^k)$

405 Recall that Γ_k is the finite set of sampled γ values at the sampling discretization level k in the
 406 computation of the embedding technique. For subsequent analysis in the paper, we make the
 407 following assumption on Γ_k .

408 **Assumption 3.1.** Assume that the sequence of finite set discretization refinements $\Gamma_k \subset (-\infty, \infty)$,
 409 $k = 1, 2, \dots$, used in the computation of the embedding technique satisfies

$$\Gamma_1 \subset \Gamma_2 \subset \dots \subset \Gamma_k \subset \Gamma_{k+1} \subset \dots \quad (3.26)$$

410 In addition, for any fixed γ_* , there exists a monotonically increasing sequence $\{\gamma_{i_k}\}$, where $\gamma_{i_k} \in \Gamma_k$
 411 and $\gamma_{i_k} \leq \gamma_*$, such that

$$\lim_{k \rightarrow \infty} \gamma_{i_k} = \gamma_* .$$

412 **Remark 3.3.** It is straightforward to construct a sequence of discretization refinements Γ_k satisfy-
 413 ing Assumption 3.1. As an example, we consider the following uniform discretization refinements
 414 when going from level k to level $k + 1$.

415 (1). Add new fine grid nodes between every two coarse grid nodes in Γ_k .

416 (2). Set $\max(\Gamma_{k+1}) = 2 * \max(|\max(\Gamma_k)|, |\min(\Gamma_k)|)$,

417 (3). Set $\min(\Gamma_{k+1}) = -2 * \max(|\max(\Gamma_k)|, |\min(\Gamma_k)|)$.

418 Next we investigate the asymptotic property of $\mathcal{S}((\mathcal{Y}_Q^\dagger)^k)$. Recall that the set $\mathcal{S}((\mathcal{Y}_Q^\dagger)^k)$ is the
 419 union of $\mathcal{S}_\mu((\mathcal{Y}_Q^\dagger)^k)$ for all positive μ where

$$\mathcal{S}_\mu((\mathcal{Y}_Q^\dagger)^k) = \{(\mathcal{V}_*, \mathcal{E}_*) \in (\mathcal{Y}_Q^\dagger)^k : \mu\mathcal{V}_* - \mathcal{E}_* = \inf_{(\mathcal{V}, \mathcal{E}) \in (\mathcal{Y}_Q^\dagger)^k} \mu\mathcal{V} - \mathcal{E}\}. \quad (3.27)$$

420 **Lemma 3.8.** Assume $\mathcal{S}_\mu(\mathcal{Y}_Q^\dagger) \neq \emptyset$ at $\mu = \mu_0$. Let $(\mathcal{Y}_Q^\dagger)^k$ be computed using the finite refinement
 421 Γ_k , where Γ_k satisfies Assumption 3.1. Then

$$\lim_{k \rightarrow \infty} \left(\inf_{(\mathcal{V}, \mathcal{E}) \in (\mathcal{Y}_Q^\dagger)^k} (\mu_0 \mathcal{V} - \mathcal{E}) \right) = \inf_{(\mathcal{V}, \mathcal{E}) \in \mathcal{Y}_Q^\dagger} (\mu_0 \mathcal{V} - \mathcal{E}). \quad (3.28)$$

422 *Proof.* Following Lemma 3.1, there exists $(\mathcal{V}^{\min}(\mu_0), \mathcal{E}^{\min}(\mu_0)) \in \mathcal{S}_{\mu_0}(\mathcal{Y}_Q^\dagger)$. Let

$$\begin{aligned} f &= \inf_{(\mathcal{V}, \mathcal{E}) \in \mathcal{Y}_Q^\dagger} (\mu_0 \mathcal{V} - \mathcal{E}), \\ f_k &= \inf_{(\mathcal{V}, \mathcal{E}) \in (\mathcal{Y}_Q^\dagger)^k} (\mu_0 \mathcal{V} - \mathcal{E}). \end{aligned} \quad (3.29)$$

423 From (3.2) and (3.26),

$$f_k \geq f, \quad \text{and} \quad f_{k+1} \leq f_k.$$

424 Hence, $\lim_{k \rightarrow \infty} \left(\inf_{(\mathcal{V}, \mathcal{E}) \in (\mathcal{Y}_Q^\dagger)^k} (\mu_0 \mathcal{V} - \mathcal{E}) \right) = \lim_{k \rightarrow \infty} f_k$ exists .

425 Next, we prove that (3.28) holds by contradiction. Suppose (3.28) does not hold. Since $f_k \geq f$,
 426 $\forall k$, and f_k is monotonically decreasing, it follows that $\exists \epsilon > 0$ s.t.

$$f < f_k - \epsilon, \quad \forall k,$$

427 which implies that

$$f \leq \left(\inf_{(\mathcal{V}, \mathcal{E}) \in (\mathcal{Y}_Q^\dagger)^k} (\mu_0 \mathcal{V} - \mathcal{E}) \right) - \epsilon, \quad \forall k. \quad (3.30)$$

428 From Lemma 3.4, there exists $\gamma^{\min}(\mu_0)$ such that

$$\gamma^{\min}(\mu_0) = \frac{1}{\mu_0} + 2\mathcal{E}^{\min}(\mu_0).$$

429 From Assumption 3.1, there exists a monotonically increasing sequence $\{\gamma_k\}$ such that

$$\lim_{k \rightarrow \infty} \gamma_k = \gamma^{\min}(\mu_0), \quad \gamma_k \in \Gamma_k .$$

430 By Lemma 3.6, there exists a sequence $\{\mu_k\}$ and corresponding sequence $\{\gamma_k = \gamma^{\min}(\mu_k)\}$, $\gamma_k \in \Gamma_k$,
 431 such that

$$(\mathcal{V}^{\min}(\mu_k), \mathcal{E}^{\min}(\mu_k)) \in \mathcal{S}_{\mu_k}(\mathcal{Y}_Q^\dagger) ,$$

432 and

$$\lim_{k \rightarrow \infty} (\mathcal{V}^{\min}(\mu_k), \mathcal{E}^{\min}(\mu_k)) = (\mathcal{V}^{\min}(\mu_0), \mathcal{E}^{\min}(\mu_0)).$$

433 From Lemma 3.4, note that

$$(\mathcal{V}^{\min}(\mu_k), \mathcal{E}^{\min}(\mu_k)) \in \mathcal{S}_{\mu_k}(\mathcal{Y}_Q^\dagger) = \mathcal{Y}_{Q(\gamma^{\min}(\mu_k))}^\dagger \subset (\mathcal{Y}_Q^\dagger)^k . \quad (3.31)$$

434 Since $(\mathcal{V}^{\min}(\mu_0), \mathcal{E}^{\min}(\mu_0)) \in \mathcal{S}_{\mu_0}(\mathcal{Y}_Q^\dagger)$, we have

$$\mu_0 \mathcal{V}^{\min}(\mu_0) - \mathcal{E}^{\min}(\mu_0) = \inf_{(\mathcal{V}, \mathcal{E}) \in \mathcal{Y}_Q^\dagger} \mu_0 \mathcal{V} - \mathcal{E} .$$

435 In other words, there exists a sequence of points (noting equation (3.31))

$$(\mathcal{V}_k, \mathcal{E}_k) = (\mathcal{V}^{\min}(\mu_k), \mathcal{E}^{\min}(\mu_k)) \in (\mathcal{Y}_Q^\dagger)^k$$

436 such that

$$\lim_{k \rightarrow \infty} \mu_0 \mathcal{V}_k - \mathcal{E}_k = \inf_{(\mathcal{V}, \mathcal{E}) \in \mathcal{Y}_Q^\dagger} \mu_0 \mathcal{V} - \mathcal{E} = f,$$

437 which contradicts (3.30). □

438 Now we establish an asymptotic property for $\mathcal{S}((\mathcal{Y}_Q^\dagger)^k)$.

439 **Theorem 3.1.** *Let $(\mathcal{Y}_Q^\dagger)^k$ be computed using the finite refinement Γ_k of γ , where Γ_k satisfies*
 440 *Assumption 3.1. Assume that $\mathcal{S}_\mu(\mathcal{Y}_Q^\dagger) \neq \emptyset$ for some $\mu > 0$. Let $(\mathcal{V}_k, \mathcal{E}_k) \in \mathcal{S}_\mu((\mathcal{Y}_Q^\dagger)^k)$. Let*
 441 *$(\mathcal{V}_*, \mathcal{E}_*)$ be a limit point of $\{(\mathcal{V}_k, \mathcal{E}_k)\}$. Then $(\mathcal{V}_*, \mathcal{E}_*) \in \mathcal{S}_\mu(\mathcal{Y}_Q^\dagger)$. If $\mathcal{S}_\mu(\mathcal{Y}_Q^\dagger)$ is a singleton, i.e.,*
 442 *$\mathcal{S}_\mu(\mathcal{Y}_Q^\dagger) = \{(\mathcal{V}_*, \mathcal{E}_*)\}$, then $\{(\mathcal{V}_k, \mathcal{E}_k)\}$ converges to $(\mathcal{V}_*, \mathcal{E}_*)$.*

443 *Proof.* Since $(\mathcal{Y}_Q^\dagger)^k \subseteq \mathcal{Y}_Q^\dagger$, $(\mathcal{V}_k, \mathcal{E}_k) \in \mathcal{Y}_Q^\dagger$. By Lemma 3.8, we have

$$\mu \mathcal{V}_* - \mathcal{E}_* = \lim_{k \rightarrow \infty} \mu \mathcal{V}_k - \mathcal{E}_k = \inf_{(\mathcal{V}, \mathcal{E}) \in \mathcal{Y}_Q^\dagger} \mu \mathcal{V} - \mathcal{E}.$$

444 Hence, any limit point $(\mathcal{V}_*, \mathcal{E}_*)$ of $\{(\mathcal{V}_k, \mathcal{E}_k)\}$ is in $\mathcal{S}(\mathcal{Y}_Q^\dagger)$. If $\mathcal{S}_\mu(\mathcal{Y}_Q^\dagger)$ is a singleton, it follows that
 445 $\{(\mathcal{V}_k, \mathcal{E}_k)\}$ converges to $\{(\mathcal{V}_*, \mathcal{E}_*)\} = \mathcal{S}_\mu(\mathcal{Y}_Q^\dagger)$. □

446 **Remark 3.4.** *Theorem 3.1 implies that every limit point of a sequence in $\mathcal{S}_\mu((\mathcal{Y}_Q^\dagger)^k)$ converges to a point in $\mathcal{S}_\mu(\mathcal{Y}_Q^\dagger)$ as the refinement level $k \rightarrow +\infty$. However, the converse is not true in general. More specifically, there may exist points in $\mathcal{S}_\mu(\mathcal{Y}_Q^\dagger)$ which are not a limit point of $\{\mathcal{S}_\mu((\mathcal{Y}_Q^\dagger)^k)\}$. This can occur if there are three or more points in $\mathcal{S}_\mu(\mathcal{Y}_Q^\dagger)$ for a fixed μ . In this case, only two of these points certainly are limit points of points in $\mathcal{S}_\mu((\mathcal{Y}_Q^\dagger)^k)$. In Figure 3.1, a pictorial illustration of this case is presented. In this illustration, for a fixed μ , there are five points in $\mathcal{S}_\mu(\mathcal{Y}_Q^\dagger)$, only two of which, namely the first and the fifth (from left to right), are certain to be limit points of points in $\mathcal{S}_\mu((\mathcal{Y}_Q^\dagger)^k)$.*

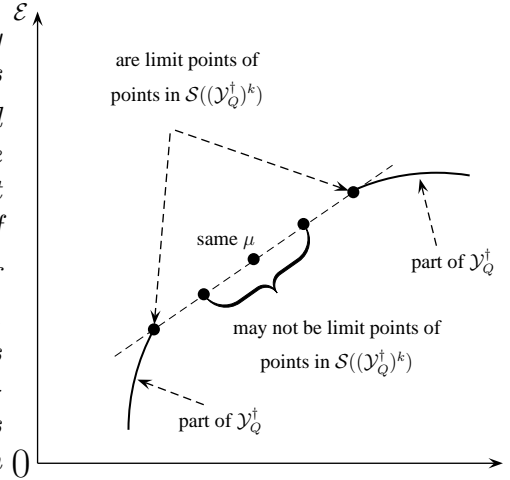


FIGURE 3.1: An illustration of situations where there exist points in $\mathcal{S}_\mu(\mathcal{Y}_Q^\dagger)$ which may not be limit points of points in $\mathcal{S}_\mu((\mathcal{Y}_Q^\dagger)^k)$.

447 **4 An MV optimal asset-liability example**

448 In this section, we illustrate, using an MV optimal asset-liability example, the asymptotic relation-
 449 ship of the solution set $\mathcal{S}((\mathcal{Y}_Q^\dagger)^k)$ corresponding to a sampling of embedding parameter Γ_k and the
 450 solution set $\mathcal{S}(\mathcal{Y}_Q^\dagger)$ corresponding to the full embedding parameter $(-\infty, +\infty)$.

451 We consider an MV asset allocation problem in which an investor dynamically adjusts positions
 452 in a risk-free asset, e.g. a bond, and a risky asset, e.g. a stock, to maximize the expected wealth of
 453 the investment portfolio, given a target level of risk. We refer the reader to [7, 21, 25, 28, 29, 33]
 454 and references therein, for a more detailed discussion on MV portfolio allocation.

455 It is common for investment institutions, such as pension funds or banks, to incorporate li-
 456 abilities into portfolio allocation decisions. These asset-liability problems can be formulated as
 457 a multi-criteria MV optimization problem. This problem can then be solved via the embedding
 458 technique [31].

459 In our illustrating example, we focus on a typical case of an asset-liability problem under MV
 460 criteria where (a) the underlying risky asset follows a jump-diffusion, and (b) the liabilities are of
 461 the form of deterministic cash outflows. As a concrete example, we can consider the problem faced
 462 by a university endowment which is invested in risky assets, yet must fund fixed cash flows each
 463 year (e.g., an endowed chair).

464 More specifically, at each instant of a pre-determined set of dates, the investor (i) first withdraws
 465 an amount, subject to certain inflation rate, from the risk-free asset, and (ii) then rebalances the
 466 portfolio. We assume in the following that there is a leverage constraint and that trading must
 467 immediately cease if the investor is insolvent. We refer readers to [13] for discussions of constraints
 468 on (continuous time) MV portfolio allocation.

469 **4.1 Underlying processes**

470 We denote by S_t and B_t the *amounts* invested in the risky and the risk-free assets, respectively.
 471 For use later in the paper, define $t^- = t - \epsilon$, $t^+ = t + \epsilon$, where $\epsilon \rightarrow 0^+$, i.e. t^- and t^+ respectively
 472 are instants of time just before and after the (forward) time t .

473 Under the objective measure, assume that S_t follows the process

$$\frac{dS_t}{S_{t^-}} = (\eta - \lambda\kappa)dt + \sigma dZ_t + d\left(\sum_{i=1}^{\pi_t} (\xi_i - 1)\right), \quad (4.1)$$

474 where dZ_t is the increment of a Wiener process, η is the real world drift rate, and σ is the volatility.
 475 In addition, π_t is a Poisson process with positive intensity parameter λ , and ξ_i are independent and
 476 identically distributed positive random variables having distribution (4.2). When a jump occurs,
 477 we have $S_{t^+} = \xi_i S_{t^-}$. As a specific example, consider ξ following a log-normal distribution $p(\xi)$
 478 given by [24]

$$p(\xi) = \frac{1}{\sqrt{2\pi}\zeta\xi} \exp\left(-\frac{(\log(\xi) - \nu)^2}{2\zeta^2}\right), \quad (4.2)$$

479 with parameters ζ and ν . We have $E[\xi] = \exp(\nu + \zeta^2/2)$, where $E[\cdot]$ denotes the expectation
 480 operator, and $\kappa = E[\xi] - 1$.

481 We assume the dynamics of the risk-free asset B_t follows

$$dB_t = rB_t dt, \quad (4.3)$$

482 where r is the risk-free rate. We make the assumption that $\eta > r$, hence, it is never optimal
 483 (in an MV setting) to short stock. As a result, the amount invested in the risky asset is always
 484 nonnegative, i.e. $S_t \geq 0$. However, we allow short positions in the risk-free asset, i.e. it is possible
 485 that $B_t < 0$.

486 We consider the set of pre-determined times, referred to as *event times*,

$$t_1 < \dots < t_M = T, \quad (4.4)$$

487 where T denotes the time horizon of the investment. We also denote by $t_0 = 0$ the inception
 488 time of the investment. We assume that there is no withdrawal at time t_0 . At each event time t_i ,
 489 $i = 1, \dots, M$, the investor (i) first withdraws an amount of cash, denoted by a_i , from the risk-free
 490 asset, and (ii) then rebalances the portfolio. Here, the withdrawal amount a_i at the event time t_i is
 491 computed by $a_i = a(t_i - t_{i-1})e^{f \times t_i}$, where a is the (continuous) constant withdrawal rate, $t_i - t_{i-1}$
 492 denotes the time interval between two event times t_i and t_{i-1} , and f is a (constant) inflation rate.

493 4.2 Liquidation value

494 In the remainder of the paper, let $X_t = (S_t, B_t)$ denote the multi-dimensional process and $x = (s, b)$
 495 denote the state of the system. We denote by $W_t \equiv W(S_t, B_t) = S_t + B_t$, $t \leq T$, the total liquidation
 496 value at time t of the investor's portfolio. For use later in the paper, we define the solvency region,
 497 denoted by \mathcal{N} , as

$$\mathcal{N} = \{(s, b) \in [0, \infty) \times (-\infty, +\infty) : W(s, b) > 0\}. \quad (4.5)$$

498 The bankruptcy (insolvency) region, denoted by \mathcal{B} , is defined as

$$\mathcal{B} = \{(s, b) \in [0, \infty) \times (-\infty, +\infty) : W(s, b) \leq 0\}. \quad (4.6)$$

499 4.3 Computing $(\mathcal{Y}_Q^\dagger)^k$

500 Recall that $(\mathcal{Y}_Q^\dagger)^k = \bigcup_{\gamma_{i_k} \in \Gamma_k} \mathcal{Y}_{Q(\gamma_{i_k})}^\dagger$, where Γ_k is the finite discrete set of sampled γ values at the
 501 sampling discretization level k . For a given $\gamma = \gamma_{i_k} \in \Gamma_k$, the MV point $\mathcal{Y}_{Q(\gamma_{i_k})}^\dagger$ in the computed
 502 MV embedded objective set $(\mathcal{Y}_Q^\dagger)^k$ of the above-described asset-liability problem can be determined
 503 as described below.

504 Let $\tau = T - t$, and $\tau_j = T - t_i$, $i = 0, \dots, M$, $j = M - i$, be the time to maturity at the
 505 i th event time. Here, $\tau_0 = T$ and $\tau_M = 0$. In addition, for use later in the paper, we denote by
 506 $\tau_j^+ = \tau_j + \epsilon$, where $\epsilon \rightarrow 0^+$. We denote by \bar{a}_j , $k = 0, \dots, M - 1$, the withdrawal amount in terms
 507 of the backward time variable τ . Then, we have

$$\bar{a}_j = a(\tau_{j+1} - \tau_j)e^{f(T-\tau_j)}, \quad j = 0, \dots, M - 1.$$

508 We further denote by c_j , $j = 0, \dots, M - 1$, the control variable representing the amount of the
 509 risk-free asset after the rebalancing of the portfolio at the event time τ_j has been carried out; c_j
 510 can take any value in $\mathcal{Z} = (-\infty, +\infty)$.

511 **4.3.1 Value function**

512 Define the value function $V(s, b, \tau)$ as

$$V(s, b, \tau) = \inf_{c(\cdot)} \left\{ E_{c(\cdot)}^{x,t} \left[(W_T - \frac{\gamma}{2})^2 \right] \right\}, \quad (4.7)$$

513 which, apart from the constant factor $\gamma^2/4$, is the objective function in equation (2.8). In addition,
514 we define the following operators

$$\begin{aligned} \mathcal{L}V &\equiv \frac{\sigma^2 s^2}{2} V_{ss} + (\eta - \lambda \kappa) s V_s + r b V_b - \lambda V, \\ \mathcal{J}V &\equiv \int_0^\infty p(\xi) V(\xi s, b, \tau) d\xi. \end{aligned} \quad (4.8)$$

515 **Rebalancing/liquidation conditions and an associated PIDE.** At time $\tau = \tau_j$, $j =$
516 $0, \dots, M - 1$, we enforce the following conditions:

517 (1) If $(s, b) \in \mathcal{B}$, we enforce the liquidation condition

$$V(s, b, \tau_j^+) = V(0, W(s, b) - \bar{a}_j, \tau_j). \quad (4.9)$$

518 (2) If $(s, b) \in \mathcal{N}$, we enforce the rebalancing optimality condition

$$\begin{aligned} V(s, b, \tau_j^+) &= \min_{c_j \in \mathcal{Z}} V(S^+, B^+, \tau_j) \\ S^+ &= s + b - \bar{a}_j - c_j \quad ; \quad B^+ = c_j \end{aligned} \quad (4.10)$$

519 subject to the leverage condition

$$\frac{S^+}{S^+ + B^+} \leq q_{\max} \quad (4.11)$$

520 where q_{\max} is a known constant with a typical value in $[1.5, 2.0]$. Note that, for the special
521 case of τ_0 , we have $V(s, b, \tau_0) = \left(W(s, b) - \frac{\gamma}{2} \right)^2$.

522 Within each time period $(\tau_j^+, \tau_{j+1}]$, $j = 0, \dots, M - 1$, we have

523 (1) If $(s, b) \in \mathcal{B}$, we enforce the liquidation condition

$$V(s, b, \tau) = V(0, W(s, b), \tau). \quad (4.12)$$

524 (2) If $(s, b) \in \mathcal{N}$, $V(s, b, \tau)$ satisfies the Partial Integro-Differential Equation (PIDE)

$$V_\tau = \mathcal{L}V + \mathcal{J}V, \quad (4.13)$$

525 subject to the initial condition (4.10).

526 **Localization.** The domain for conditions (4.9)-(4.12) and the PIDE (4.13) is $(s, b, \tau) \in \Omega_j^\infty \equiv$
527 $[0, \infty) \times (-\infty, +\infty) \times [\tau_j^+, \tau_{j+1}]$. For computational purposes, we localize this domain to the set of
528 points

$$(s, b, \tau) \in \Omega_j = [0, s_{\max}) \times [-b_{\max}, b_{\max}] \times [\tau_j^+, \tau_{j+1}], \quad (4.14)$$

529 where s_{\max} and b_{\max} are sufficiently large positive numbers (and are the same for all event time
530 periods). Let $s^* < s_{\max}$. Following [13], we define the following computational sub-domains:

$$\begin{aligned} \Omega_{s_0} &= \{0\} \times [-b_{\max}, b_{\max}] \times [\tau_j^+, \tau_{j+1}], \quad \Omega_{s^*} = (s^*, s_{\max}) \times [-b_{\max}, b_{\max}] \times [\tau_j^+, \tau_{j+1}], \\ \Omega_{\mathcal{B}} &= \{(s, b, \tau) \in \Omega_j \setminus \Omega_{s_0} \setminus \Omega_{s^*} : W(s, b) \leq 0\}, \quad \Omega_{in} = \Omega_j \setminus \Omega_{s_0} \setminus \Omega_{s^*} \setminus \Omega_{\mathcal{B}}, \\ \Omega_{b_{\max}} &= (0, s^*] \times [-b_{\max}e^{rT}, -b_{\max}) \cup (b_{\max}, b_{\max}e^{rT}] \times [\tau_j^+, \tau_{j+1}]. \end{aligned}$$

531 At time $\tau = \tau_j$, we enforce (i) the liquidation condition (4.9) in $\Omega_{\mathcal{B}}$, and (ii) the optimality condition
532 (4.10) in Ω_{in} . Within each time period $(\tau_j^+, \tau_{j+1}]$, $j=0, \dots, M-1$, we have the following localized
533 problem:

$$\begin{aligned} V_\tau &= rbV_b, \quad (s, b, \tau) \in \Omega_{s_0}; \\ V_\tau &= (\sigma^2 + 2\eta + \lambda\kappa_2)V, \quad (s, b, \tau) \in \Omega_{s^*}, \quad \text{where } \kappa_2 = E[(J-1)^2]; \\ V &= V(0, W(s, b), \tau), \quad (s, b, \tau) \in \Omega_{\mathcal{B}}; \\ V_\tau &= \mathcal{L}V + \mathcal{J}_\ell V, \quad (s, b, \tau) \in \Omega_{in}, \quad \text{where } \mathcal{J}_\ell V = \int_0^{s_{\max}/s} p(\xi)V(\xi s, b, \tau) d\xi; \\ V &= \left(\frac{b}{b_{\max}}\right)^2 V(s, \text{sgn}(b)b_{\max}, \tau), \quad (s, b, \tau) \in \Omega_{b_{\max}}. \end{aligned} \quad (4.15)$$

534 Some guidelines for choosing s^* , s_{\max} which minimize the effect of the localization error for the jump
535 terms can be found in [16]. We refer the reader to [13] for relevant details regarding a derivation
536 of (4.15).

537 We numerically solve the localized problem (4.15) using finite differences with a semi-Lagrangian
538 timestepping method as described in [13].

539 4.3.2 Expected value problem.

540 We denote by $c_\gamma^*(\cdot)$ the optimal control of problem (4.7). Once we have determined $c_\gamma^*(\cdot)$, we use
541 this control to determine

$$E_{c_\gamma^*}^{x,t}[W_T], \quad (4.16)$$

542 since this information is needed in order to determine the corresponding MV embedded point. This
543 step essentially involves solving an associated linear PIDE over each event time period $[\tau_j, \tau_{j+1}]$,
544 $k=0, \dots, M-1$, details of which are similar to those described in [13], and hence, are omitted.

545 Using numerical solutions for equations (4.7) and (4.16) at the event time $\tau_M = t_0$, we then
546 compute the embedded MV point

$$\mathcal{Y}_{Q(\gamma)}^\dagger \equiv \{(V_\gamma^*, \mathcal{E}_\gamma^*)\} = \left\{ (Var_{c_\gamma^*(\cdot)}^{x_0,0}[W_T], E_{c_\gamma^*(\cdot)}^{x_0,0}[W_T]) \right\}. \quad (4.17)$$

547 Repeating the above-mentioned procedure for all different values of $\gamma \in \Gamma_k$ yields the computed
548 MV embedded set $(\mathcal{Y}_Q^\dagger)^k$.

r	σ	η	ν	λ	ζ	$W(0)$	a	f	q_{\max}	T	$\Delta\tau$
.0445	0.1765	.0795	-.7883	.0585	.4505	100.	6.	0.03	1.5	20. (yrs)	1. (yr)

TABLE 4.1: *Parameter values for the MV asset-liability example*

Refine level (k)	Timesteps	s nodes	b nodes	γ nodes	γ_{\min}	γ_{\max}
0	30	62	30	75	-0.5×10^5	-0.5×10^5
1	60	123	59	151	-1×10^5	1×10^5
2	120	245	117	303	-2×10^5	2×10^5

TABLE 4.2: *Computational grid for solving the PIDE (4.13). We refer the reader to [13] for more details.*

549 4.4 Numerical results

550 Recall that $(\mathcal{Y}_Q^\dagger)^k$, computed using Γ_k , is an approximation to \mathcal{Y}_Q^\dagger . Once we obtain $(\mathcal{Y}_Q^\dagger)^k$ for a given
551 Γ_k , we then apply the post-processing method described in Algorithm 3.1 to $(\mathcal{Y}_Q^\dagger)^k$ to determine
552 $\mathcal{S}((\mathcal{Y}_Q^\dagger)^k)$. As shown in Section 3, if convergence occurs, this process provides an increasingly
553 accurate estimate of $\mathcal{S}(\mathcal{Y}_Q^\dagger)$ as k increases. We illustrate this by the MV asset-liability example
554 described in the previous section. Table 4.1 summarizes the parameter values in our example. We
555 carry out experiments with three levels of refinement, details of which are in Table 4.2.

556 **Remark 4.1** (Combination of refinements of Γ_k and of the PIDE grid). *Suppose we denote the*
557 *discretization parameter of the PIDE by h , which is inversely proportional to numbers of timesteps,*
558 *s and b nodes. If we fix h , then we should observe convergence of $(\mathcal{S}(\mathcal{Y}_Q^\dagger)^k)_h$ to $(\mathcal{S}(\mathcal{Y}_Q^\dagger))_h$ as Γ_k*
559 *is refined, i.e. as $k \rightarrow \infty$. However, due the finite mesh size of the PIDE grid, there is PIDE*
560 *discretization error in the numerical solutions. We should then repeat the above convergence test*
561 *for smaller values of h . In our experiments, we take the shortcut of combining the refinements of*
562 *Γ_k and of the PIDE grid. This combination is reflected in Table 4.2.*

563 **Remark 4.2** (Complexity). *Recall that $(\mathcal{Y}_Q^\dagger)^k = \bigcup_{\gamma_{i_k} \in \Gamma_k} \mathcal{Y}_{Q(\gamma_{i_k})}^\dagger$. For a given $\gamma = \gamma_{i_k} \in \Gamma_k$, the*
564 *MV point $\mathcal{Y}_{Q(\gamma_{i_k})}^\dagger$ is computed by solving the associated MV asset-liability problem as described in*
565 *Subsection 4.3. Examination of the solution steps reveals that*

- 566 • *each re-balancing timestep requires solution of the local optimization problem (4.10) at each*
567 *node.*
- 568 • *each non-rebalancing timestep requires solution of the PIDE (4.13).*

569 *At each re-balancing times τ_j , $j = 0, \dots, M - 1$, in order to solve the local optimization problems,*
570 *we discretize the control (with discretization parameter h) and the use simple linear search. We*
571 *have found that using a continuous 1-D optimization method is unreliable, and often converges to*
572 *a local, not global, minimum. Each optimization problem is resolved by evaluating the objective*
573 *function $O(1/h)$ times. Since there are $O(1/h^2)$ nodes, and $O(1)$ re-balancing timesteps, this gives*
574 *a total complexity of $O(1/h^3)$ for all re-balancing timesteps.*

575 At each non-rebalancing timestep, the fixed-point iteration developed in [16] is used, which re-
576 quires an FFT at each iteration. The total complexity at each non-rebalancing timestep is then
577 $O(1/h^2|\log h|)$, which amounts to a total complexity of $O(1/h^3|\log h|)$ for all non-rebalancing
578 timesteps. Thus, for a single γ , the total complexity is $O(1/h^3|\log h|)$.

579 **Remark 4.3** (Spurious points). *There is an obvious strategy which generates zero variance: invest*
580 *all wealth in the risk-free asset at all withdrawal times. The certain value of \mathcal{E} corresponding to*
581 *this risk-free strategy, denoted by \mathcal{E}_{rf} , can be computed by an annuity calculation. We denote by γ_{rf}*
582 *the corresponding value of γ which generates this strategy. Since this strategy has zero variance, it*
583 *can be viewed as corresponding to the case $\mu \rightarrow \infty$, i.e. infinitely risk-averse. Hence, from (2.14),*
584 *it follows that $\gamma_{rf} = 2\mathcal{E}_{rf}$. This value γ_{rf} should be the smallest possible value of γ which can*
585 *generate a valid point in $\mathcal{S}(\mathcal{Y}_Q^\dagger)$. However, as noted in Remark 2.1, a solution to the embedded*
586 *problem exists $\forall \gamma \in (-\infty, +\infty)$. Consequently, from Remark 3.2, we expect that points in $\mathcal{Y}_{Q(\gamma)}^\dagger$,*
587 *$\gamma < \gamma_{rf}$, are spurious points.*

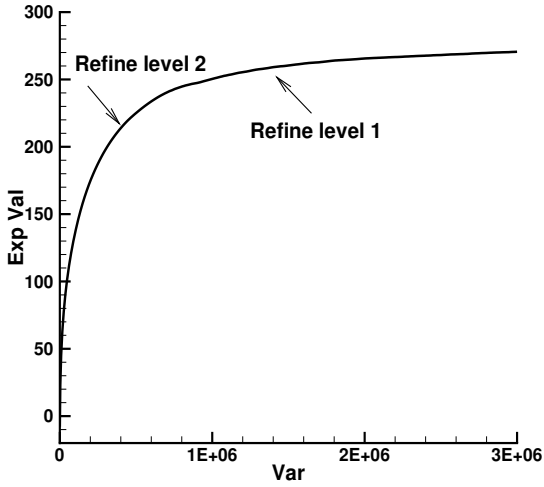
588 In Figure 4.1 (a), we present the computed MV embedded objective sets $(\mathcal{Y}_Q^\dagger)^k$, $k = 1, 2$,
589 plotted as expected value versus variance. In Figure 4.1 (b), we present the same sets, but plotted
590 as expected value versus standard deviation, which is a more practically meaningful display of the
591 results, since standard deviation and expected value have the same units. Figure 4.1 (c) shows the
592 same plot as in Figure 4.1 (b), but zoomed in the lower-left region, where we expect spurious points
593 (see Remark 4.3). We make the following observations:

- 594 • In Figures 4.1 (a) and (b), the computed MV embedded objective set $(\mathcal{Y}_Q^\dagger)^k$ for $k = 2$ visually
595 coincides with that for $k = 1$. Further refinement steps show negligible changes. This suggests
596 convergence of the numerical solution and of the efficient frontier.
- 597 • Figure 4.1 (c) indicates that the computed MV embedded objective sets $(\mathcal{Y}_Q^\dagger)^k$, $k = 1, 2$,
598 indeed contain spurious points in the lower-left region, as expected.

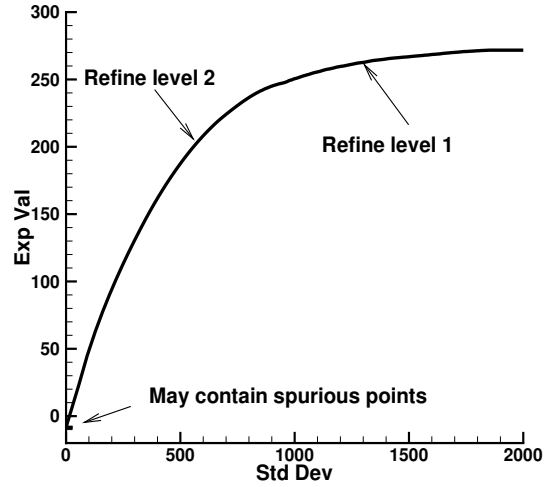
599 To remove spurious points in the computed MV embedded objective sets $(\mathcal{Y}_Q^\dagger)^k$, $k = 1, 2$, we
600 apply the post-processing method described in Algorithm 3.1. After this process, we obtain the
601 corresponding sets $\mathcal{S}((\mathcal{Y}_Q^\dagger)^k)$, which are presented in Figure 4.1 (d). Again, we emphasize the strong
602 agreement between the two levels of refinement. Based on the theoretical result of this paper and
603 the strong agreement between $\mathcal{S}((\mathcal{Y}_Q^\dagger)^k)$, $k = 1, 2$, in Figure 4.1 (d), it appears that every point in
604 the set $\mathcal{S}((\mathcal{Y}_Q^\dagger)^2)$ is indeed close to a point in the set $\mathcal{S}(\mathcal{Y}_Q^\dagger) = \mathcal{Y}_P$, and hence, is MV scalarization
605 optimal.

606 We note that, in practice, the interesting part of the efficient frontier is in the range $\gamma \in$
607 $[\gamma_{rf}, q|\gamma_{rf}|]$, with q being problem dependent, and γ_{rf} , as mentioned in Remark 4.3, is the smallest
608 γ which can generate a valid point in $\mathcal{S}(\mathcal{Y}_Q^\dagger)$. In our case, $q = 10$ proved to be a reasonable
609 parameter. With this range of values for γ , the convergence of $\mathcal{S}((\mathcal{Y}_Q^\dagger)^k)$, similar to what we
610 observed in Figure (4.1), can be obtained with only 15 γ points for $k = 1$, and 29 γ points for
611 $k = 2$.

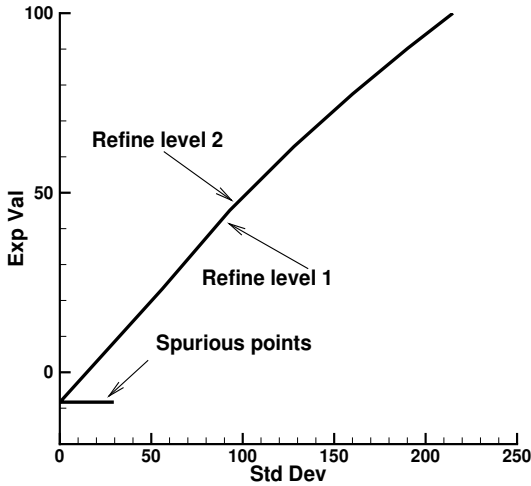
612 Theorem 3.1 states that, for fixed μ , the limit points of $\mathcal{S}_\mu((\mathcal{Y}_Q^\dagger)^k)$, $k \rightarrow \infty$, are points in
613 $\mathcal{S}_\mu(\mathcal{Y}_Q^\dagger)$. However, the convergence of this procedure will likely be highly dependent on μ . For
614 example, if μ is small (i.e. small slope of the supporting hyperplane), then the numerical results will
615 be very sensitive to small errors. To illustrate this effect, we carried out the following experiments.



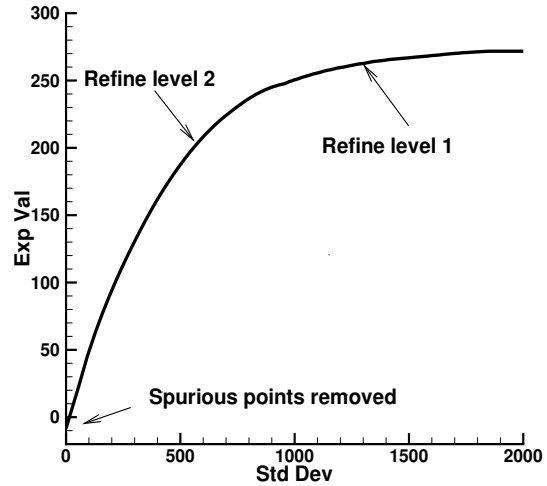
(a) $(\mathcal{Y}_Q^\dagger)^k$, $k = 1, 2$ (Expected value vs. variance)



(b) $(\mathcal{Y}_Q^\dagger)^k$, $k = 1, 2$ (Expected value vs. standard deviation)



(c) $(\mathcal{Y}_Q^\dagger)^k$, $k = 1, 2$ (Expected value vs. standard deviation - zoomed in)



(d) $S((\mathcal{Y}_Q^\dagger)^k)$, $k = 1, 2$ (Expected value vs. standard deviation)

FIGURE 4.1: Plot of $(\mathcal{Y}_Q^\dagger)^k$ and $S((\mathcal{Y}_Q^\dagger)^k)$, $k = 1, 2$, of the MV asset-liability example with parameters in Table 4.1.

616 First, we compute $(\mathcal{Y}_Q^\dagger)^k$, $k = 0, 1, 2$. We then selected fixed values of μ , which did not correspond
 617 to any of the values of $\gamma \in \Gamma_k$. Then, for the fixed values of μ , we compute $\mathcal{S}_\mu((\mathcal{Y}_Q^\dagger)^k)$. Since
 618 we have only a finite number of points in $(\mathcal{Y}_Q^\dagger)^k$, then this is easily done by exhaustive search. If
 619 $\mathcal{S}_\mu(\mathcal{Y}_Q^\dagger)^k$ is not a singleton, then we pick that element of $\mathcal{S}_\mu(\mathcal{Y}_Q^\dagger)^k$ which has the smallest variance

	$\mu = 0.1$		$\mu = 0.3$		$\mu = 0.4$	
k	$\sqrt{\mathcal{V}_k^{\min}}$	\mathcal{E}_k^{\min}	$\sqrt{\mathcal{V}_k^{\min}}$	\mathcal{E}_k^{\min}	$\sqrt{\mathcal{V}_k^{\min}}$	\mathcal{E}_k^{\min}
0	711.29	217.87	326.08	129.17	326.08	129.17
1	832.71	238.90	307.60	130.26	264.69	114.55
2	911.84	250.71	298.10	130.90	247.01	111.91

TABLE 4.3: Numerical illustration of Theorem 3.1.

620 and expectation, denoted by $(\sqrt{\mathcal{V}_k^{\min}}, \mathcal{E}_k^{\min})$. In Table 4.3, we present $(\sqrt{\mathcal{V}_k^{\min}}, \mathcal{E}_k^{\min})$ for $k = 0, 1$, and
621 2. Observe that, as expected, for moderate values of $\mu = 0.3, 0.4$, the values of mean and standard
622 deviation appear to converge somewhat faster than for the $\mu = 0.1$ case. However, from a practical
623 point of view, we can see that these errors for small μ have very little effect on the efficient frontier
624 (this corresponds to large variances), as can be seen in Figure 4.1 (a). In general, there does not
625 seem to be a consistent order of rate of convergence.

626 5 Application to higher dimensional problems

627 Our main result, Theorem 3.1, is concerned with the convergence of the discretely sampled solution
628 of equation (2.8). This result is independent of any particular numerical technique used to solve
629 the control problem (2.8).

630 However, it is of practical interest to solve the asset-liability problem with several risky assets.
631 A difficulty in this case is that in order to ensure convergence to the viscosity solution of
632 the optimal control HJB equation (4.13), we need to construct monotone discretization schemes
633 [3]. For the case of correlated risky assets, construction of such schemes is a matter of on-going
634 research. We refer the reader to [14] for a discussion of the *wide stencil* approach to this problem.

635 In addition, of course, solving the HJB PDE in higher dimensions becomes problematic, due
636 to the computational complexity. Suppose there is one risk-free asset and d risky assets. Let the
637 discretization parameter for the PIDE be h , as discussed in Remark 4.2. For simplicity, we consider
638 the case where the risky assets follow a pure diffusion process (no jumps). Then, using an argument
639 similar to that used in Remark 4.2, we find that the complexity for solving the HJB equation for
640 a single value of γ is $O(1/h^{d+2})$, which increases rapidly as d increases.

641 If x is the state vector of the system, then recall that our objective is to find the control $c(\cdot)$
642 which solves

$$V(x, \tau) = \inf_{c(\cdot)} \left\{ E_{c(\cdot)}^{x, \tau} \left[(W_T - \frac{\gamma}{2})^2 \right] \right\}. \quad (5.1)$$

643 An alternative numerical approach for determining the solution of equation (5.1) would be use a
644 Monte Carlo method. This would require formulating the control problem (5.1) as a system of
645 Backward Stochastic Differential Equations (BSDEs). Some promising results for Monte Carlo
646 methods using BSDEs in the context of control problems have been obtained recently, see for
647 example [6, 18, 26]. Theorem 3.1 can then be used when sampling the solution of equation (5.1)
648 for a finite number of values of γ . Theorem 3.1 ensures us that as the sampling mesh becomes
649 finer, the results of these Monte Carlo computations generate an accurate approximation to the
650 true efficient frontiers.

6 Conclusion

Many optimal stochastic control problems in finance can be posed in term of a continuous time MV optimization problem, which involves two conflicting objectives. Using the standard scalarization technique, this multi-criteria optimization problem can be reformulated as a single-objective MV scalarization optimization problem. The goal is to determine the original MV scalarization optimal set \mathcal{Y}_P . However, dynamic programming can not be applied to the above scalarization optimization problem, due to the presence of the variance term. To overcome this difficulty, the embedding technique of [21, 33] can be applied to determine the set of computed MV embedded objectives \mathcal{Y}_Q^\dagger , which, in general, is a superset of the original MV scalarization optimal set \mathcal{Y}_P . As a result, the MV efficient frontiers generated by the embedding technique may contain spurious points, which do not belong to the original MV scalarization optimal set \mathcal{Y}_P .

In [27], it is established that spurious points in the computed MV embedded objective set \mathcal{Y}_Q^\dagger are those which are not MV scalarization optimal with respect to \mathcal{Y}_Q^\dagger . In addition, it is established that the set of MV SOPs with respect to the computed MV embedded objective set \mathcal{Y}_Q^\dagger is identical to the original MV scalarization optimal set \mathcal{Y}_P . Based on these two results, a simple, yet effective, post processing technique is developed to eliminate spurious points in the computed MV embedded objective set \mathcal{Y}_Q^\dagger .

In the context of numerical computation, however, significant complexities remain, since it is only possible to solve the embedded problem for a finite number of values of the embedding parameter, and hence we can only obtain a finite subset of the computed MV embedded objective set \mathcal{Y}_Q^\dagger . An important question is whether or not, for sufficiently large number of sampling points of the embedding parameter, the set of SOPs with respect to the afore-mentioned finite subset of \mathcal{Y}_Q^\dagger can sufficiently well approximate the set of SOPs with respect to \mathcal{Y}_Q^\dagger .

In this paper, we establish that, for sufficiently large number of sampling points of the embedding parameter, every limit point in the set of SOPs with respect to the computed finite subset of \mathcal{Y}_Q^\dagger is a point in the set of SOPs with respect to \mathcal{Y}_Q^\dagger , and hence, is MV scalarization optimal. This result combined with the analysis and post-processing numerical method developed in [27] form a practical numerical framework for eliminating spurious points from the computed MV embedded objective set. This framework can essentially be viewed as complementing the theoretical results of the popular embedding technique developed in [21, 33] for continuous time (or multi-period) MV optimization.

References

- [1] R. Almgren. Optimal trading with stochastic liquidity and volatility. *SIAM Journal of Financial Mathematics*, 3:163–181, 2012.
- [2] A. M. Andrew. Another efficient algorithm for convex hulls in two dimensions. *Information Processing Letters*, 9:216–219, 1979.
- [3] G. Barles and P.E. Souganidis. Convergence of approximation schemes for fully nonlinear equations. *Asymptotic Analysis*, 4:271–283, 1991.
- [4] S. Basak and G. Chabakauri. Dynamic mean-variance asset allocation. *Review of Financial Studies*, 23:2970–3016, 2011.

- 691 [5] N. Bauerle. Benchmark and mean-variance problems for insurers. *Mathematical Methods of*
692 *Operations Research*, 62:159–162, 2005.
- 693 [6] C. Bender and J. Steiner. Least squares Monte Carlo for BSDEs. In R. Carmona, P. Del Moral,
694 Peng Hui, and N. Oudjane, editors, *Numerical Methods in Finance*. Springer, New York, 2012.
- 695 [7] T. Bielecki, H. Jin, S. Pliska, and X.Y. Zhou. Continuous time mean-variance portfolio selection
696 with bankruptcy prohibition. *Mathematical Finance*, 15:213–244, 2005.
- 697 [8] T. Bjork and A. Murgoci. A general theory of Markovian time inconsistent stochastic control
698 problems. Available at SSRN: <http://ssrn.com/abstract=1694759>, 2010.
- 699 [9] P. Chen and S.C.P. Yam. Optimal proportional reinsurance and investment with regime
700 switching for mean-variance insurers. *Insurance: Mathematics and Economics*, 53:871–883,
701 2013.
- 702 [10] M.C. Chiu and D. Li. Asset and liability under a continuous time mean-variance optimization
703 framework. *Insurance: Mathematics and Economics*, 39:330–355, 2006.
- 704 [11] X. Cui, J. Gao, X. Li, and D. Li. Optimal multi-period mean variance policy under no-shorting
705 constraint. *European Journal of Operational Research*, 234:459–468, 2014.
- 706 [12] C. Czichowsky and M. Schweizer. Cone-constrained continuous-time Markowitz problems.
707 *Annals of Applied Probability*, 23:764–810, 2013.
- 708 [13] D. M. Dang and P. A. Forsyth. Continuous time mean-variance optimal portfolio allocation
709 under jump diffusion: An numerical impulse control approach. *Numerical Methods for Partial*
710 *Differential Equations*, 30:664–698, 2014.
- 711 [14] K. Debrabant and E.r. Jakobsen. Semi-Lagrangian schemes for linear and fully non-linear
712 diffusion equations. *Mathematics of Computation*, 82(283):1433–1462, 2012.
- 713 [15] L. Delong and R. Gerrard. Mean-variance portfolio selection for a non-life insurance company.
714 *Mathematical Methods of Operations Research*, 66:339–367, 2007.
- 715 [16] Y. d’Halluin, P.A. Forsyth, and K.R. Vetzal. Robust numerical methods for contingent claims
716 under jump diffusion processes. *IMA Journal of Numerical Analysis*, 25:87–112, 2005.
- 717 [17] P.A. Forsyth. A Hamilton Jacobi Bellman approach to optimal trade execution. *Applied*
718 *Numerical Mathematics*, 61:241–265, 2011.
- 719 [18] E. Gobet, J.-P. Lemor, and X. Warin. A regression-based Monte Carlo method to solve
720 backward stochastic differential equations. *Annals of Applied Probability*, 15:2172–2202, 2005.
- 721 [19] R. Jose-Fombellida and J. Rincon-Zapatero. Mean variance portfolio and contribution selection
722 in stochastic pension funding. *European Journal of Operational Research*, 187:120–137, 2008.
- 723 [20] M. Leippold, F. Trojani, and P. Vanini. A geometric approach to multiperiod mean variance
724 optimization of assets and liabilities. *Journal of Economic Dynamics and Control*, 28:1079–
725 1113, 2004.

- 726 [21] D. Li and W.-L. Ng. Optimal dynamic portfolio selection: multiperiod mean variance formu-
727 lation. *Mathematical Finance*, 10:387–406, 2000.
- 728 [22] X. Li, X.Y. Zhou, and E.E.B. Lim. Dynamic mean-variance portfolio constraint selection with
729 no-shorting constraints. *SIAM Journal on Control and Optimization*, 40:1540–1555, 2002.
- 730 [23] J. Lorenz and R. Almgren. Mean-variance optimal adaptive execution. *Applied Mathematical*
731 *Finance*, 18:395–422, 2011.
- 732 [24] R.C. Merton. Option pricing when underlying stock returns are discontinuous. *Journal of*
733 *Financial Economics*, 3:125–144, 1976.
- 734 [25] B. Oksendal and A. Sulem. *Applied Control of Jump Diffusions*. Springer, 2009.
- 735 [26] M. Ruijter and C.W. Oosterlee. A Fourier-cosine method for an efficient computation of
736 solutions to BSDEs. Working paper, Centrum Wiskunde & Informatica, Amsterdam, 2013.
- 737 [27] S.T. Tse, P.A. Forsyth, and Y. Li. Preservation of scalarization optimal points in the embed-
738 ding technique for continuous time mean variance optimization. *SIAM Journal on Control and*
739 *Optimization*, 52:1527–1546, 2014.
- 740 [28] E. Vigna. On the efficiency of mean-variance based portfolio selection in defined contribution
741 pension schemes. *Quantitative finance*, 14:237–258, 2014.
- 742 [29] J. Wang and P.A. Forsyth. Numerical solution of the Hamilton-Jacobi-Bellman formulation for
743 continuous time mean variance asset allocation. *Journal of Economic Dynamics and Control*,
744 34:207–230, 2010.
- 745 [30] J. Wang and P.A. Forsyth. Comparison of mean variance like strategies for optimal asset
746 allocation problems. *International Journal of Theoretical and Applied Finance*, 15(2), 2012.
747 DOI 10.1142/S0219024912500148.
- 748 [31] S. X. Xie, Z. F. Li, and S. Y. Wang. Continuous time portfolio selection with liability: Mean-
749 variance model and stochastic LQ approach. *Insurance: Mathematics and Economics*, 42:943–
750 953, 2008.
- 751 [32] H. Yao, Y. Lai, Q. Ma, and M. Jian. Asset allocation for a DC pension fund with stochastic
752 income and mortality risk: a multi-period mean-variance framework. *Insurance: Mathematics*
753 *and Economics*, 54:84–92, 2014.
- 754 [33] X.Y. Zhou and D. Li. Continuous-time mean-variance portfolio selection: A stochastic LQ
755 framework. *Applied Mathematics and Optimization*, 42(1):19–33, 2000.